Defra/Environment Agency
Flood and Coastal Defence R&D Programme

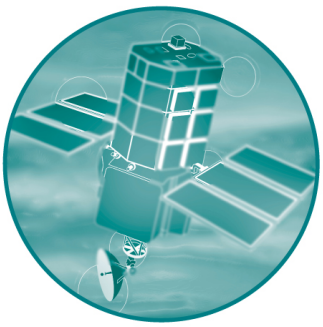

Risk Assessment for Flood & Coastal Defence for Strategic Planning

R&D Technical Report W5B-030/TR3

Intermediate Level Methodology
A Coastal Application

defra
Department for Environment Food and Rural Affairs

ENVIRONMENT AGENCY

Defra / Environment Agency
Flood and Coastal Defence R&D Programme

Risk Assessment for Flood & Coastal Defence for Strategic Planning

Intermediate Level Methodology
A Coastal Application

Report No W5B-030/TR3

June 2004

Publishing organisation

Defra
c/o RCEG
Ceres House, 2 Searby Road,
LINCOLN, LN2 4DW

Peter Allen - Williams,
R & D Coordinator, Flood Management Division,
Tel: 01522 528297 (GTN 6209 224)
Email: peter.allen-williams@defra.gsi.gov.uk

Statement of use
This document provides information for Defra and Environment Agency Staff about consistent standards for flood defence and constitutes an R&D output from the Joint Defra / Environment Agency Flood and Coastal Defence R&D Programme.

Contract Statement
This report describes work commissioned by the Environment Agency through the Risk Evaluation and Understanding of Uncertainty (REUU) Theme of the joint Defra/Environment Agency research programme. The REUU Theme Leader is Ian Meadowcroft of the Environment Agency. The appointed REUU Theme project representative was Mr Ishaq Tauqir, WS Atkins Consultants Limited. The HR Wallingford job number was CDS 0800. The work was carried out by members of the Project Team which was constructed from the following organisations: HR Wallingford Ltd (Engineering Systems and Management Group), University of Bristol (Department of Civil Engineering), Halcrow Maritime, and John Chatterton Associates. The Project Manager was Paul Sayers of HR Wallingford.

GLOSSARY OF TERMS AND ACRONYMS

Term	Definition
CG	Condition Grade, A visual assessment of the condition of a flood defence
EA	The Environment Agency of England and Wales
GIS	Geographical Information System
Pf	Probability of failure
$P(OT\|x)$	Conditional probability of overtopping given a loading *x*
$P(B\|x)$	Conditional probability of breaching given a loading *x*
$P(B\|x, CG=1\text{-}5)$	Conditional probability of breaching given a loading *x* and condition grade of 1-5
SoP	Standard of Protection
SVFI	Social Vulnerability Flood Index

SUMMARY

Driven by a need for improved management of the defences protecting the highly developed floodplains of England and Wales, an efficient systems-based risk assessment methodology has been developed. The approach calculates the risk associated with systems of defences protecting low-lying land. The complex nature of the floodplain topography in England and Wales means that significant computational expense is required to obtain realistic estimates of inundation depth and extent. The risk assessment methodology is novel in that it uses Monte Carlo methods to estimate defence responses to a large number of loading conditions. Importance sampling techniques are a proven approach to efficiently estimating the probability of failure, rather than risk which is of interest to the decision-maker. A risk-based methodology has been developed and is presented in this report with the support of an example implementation in Towyn, North Wales. This area is defended by extensive coastal defences.

This case study demonstrates that risk is a complex function of joint loadings, beach response, defence resistance, floodplain topography and the geographical location of impacts in the floodplain. The application of this rigorous level III approach allows decision-makers to obtain a deep understanding of the system, its vulnerabilities, the most efficient means of allocating resource and how it may respond to future perturbations from external activities.

For further information please contact Paul Sayers of HR Wallingford.

CONTENTS

Tables

Figures

Appendices

1. INTRODUCTION

Quantitative methods for coastal flood risk assessment have been well developed (see for example CUR and TAW, 1990, Casciati, 1992, Vrijling, 1993, Meadowcroft *et al.,*1996, USACE, 1996, Moser, 1997, Reeve, 1998, Voortman, 2003, Zerger *et al*., 2002, Hall *et al*., 2003*a*, 2003*b*). However, the behaviour under extreme conditions of defences against coastal erosion and flooding is still only partially understood. In addition, for strategic flood risk management *systems* of defences and impacts have to be considered; a given coastal floodplain may be protected by a number of different defences, whose collective integrity needs to be analysed. A significant advance in effective management of coastal risks is achievable by taking a more explicitly systems based approach. This system includes development control; the construction, operation and maintenance of flood defences; flood forecasting and warning; management of beach and cliff erosion; and management of internal drainage systems (Hall *et al*., 2003). Moreover, sediments on beaches and in coastal waters provide a mechanism of interaction between different defence sections. The behaviour of beaches is a key determinant of the reliability of coastal defences because beaches have a critical role in modifying incident waves and because toe scour is a critical failure mechanism. Strategic and planning appraisal of coastal options must therefore in some way take account of these interactions.

Methods of reliability analysis have been classified into three levels (JCSS, 1981). In level III methods, the integral of the joint probability density function (j.p.d.f.) that describes the random input variables is solved numerically. For level II methods, the failure surface is approximated by a hyperplane tangential to the failure point closest to the origin (often known as the 'design point'), after the j.p.d.f. describing the random input variables has been transformed into independent normally distributed variables. The focus of previously proposed methods for flood risk assessment has been the appraisal and design of individual schemes on the coast based on level II methods. This paper proposes a level III approach; because of the considerable data and computational requirements, until recently it has not been possible to apply these methods at a broad scale. Recently developed joint probability methods (Hawkes *et al*., 2002) and response models do not lend themselves to level II reliability analysis, but are more suited to level III analysis. Whilst level III approaches are more robust and more flexible than level II methods, for complex systems (such as a coastal defence system) they need to be efficiently implemented in order to be computationally feasible. Importance sampling techniques (Melchers, 1989, 1999) are a proven approach, but focus on accurately estimating the *probability* of system failure as opposed to *risk*. The conditions resulting in the greatest probability of failure do not necessarily result in the greatest flood risk: a weak flood defence protecting scrubland may be likely to fail, but will contribute little towards flood risk, conversely failure of a strong defence defending a city may contribute greatly towards flood risk. The complex topography of UK coastal floodplains means that significant computational time is required to model inundation in order to obtain realistic estimates of the impacts of flooding. However, this step is the most computationally expensive part of the risk assessment. A risk-based importance sampling method, described in the following section, is therefore proposed.

2. OVERVIEW OF METHODOLOGY

Flood risk is often expressed in terms of an expected annual damage, EAD, (sometimes this is referred to as the average annual damage) and traditionally defined as the product of the probability of flooding and the consequential damage. The probability of flooding is a function of defence resistance and loads. Defence strength is described probabilistically using fragility curves (Dawson and Hall, 2002*a*, 2002*b*). Joint loading conditions of wave heights and water levels are estimated using joint probability methods (Hawkes *et al*., 2002). The extent and depth of flooding resulting from this failure are estimated using an inundation model. Consequences can be calculated based on the extent and depth of flooding from the inundation model. The steps of the methodology, shown in Figure 2.1, are described in following sections.

The research described in this paper is clearly related to recent work in the Netherlands analysing and optimising the risk associated with systems of defences (Voortman *et al*., 2002) but is methodologically different, being based entirely on Monte Carlo (level III) reliability analysis. This enables the behaviour of the system to be modelled over an entire range of joint loadings, rather than be considered only under a 'design' loading. Furthermore, the complex topography of UK coastal floodplains means that more emphasis on flood inundation modelling is required in order to generate realistic estimates of flood depth and hence damage. This differs to the approach of (Voortman *et al*. 2002), where a 'bathtub' assumption of the depth of inundation could be made.

The risk assessment methodology is based on use of importance sampling in order to reduce the computational resources required to estimate flood risk. The approach is novel in that the joint space of the loading variables (wave height and water level) is sampled according to the contribution that a given sub-region of that space makes to *risk*. This is different to the conventional importance sampling approach, widely used in structural reliability analysis (Melchers, 1989, 1999), where the joint space is sampled according to the contribution towards the *probability of failure*. The task is not, however, straightforward as in order to obtain an estimate of flood damage (and hence contribution to risk) for floodplains of any complexity (i.e. where a bathtub inundation model is inappropriate) it is necessary to model flood inundation, which is usually a computationally expensive task. Whilst the flood risk assessment methodology is not dependent on the use of a specific hydrodynamic model, in the example implementation described later in this paper, some of this computational expense is relieve by using a fast raster-based 2D flood inundation model called LISFLOOD (Bates and De Roo, 2000) for which of the order of 1000s of flood simulations can be conducted in reasonable computational time. Even this number of model realisations is not great in comparison to the number of possible realisations in a system of moderate complexity, so an efficient sampling methodology is required.

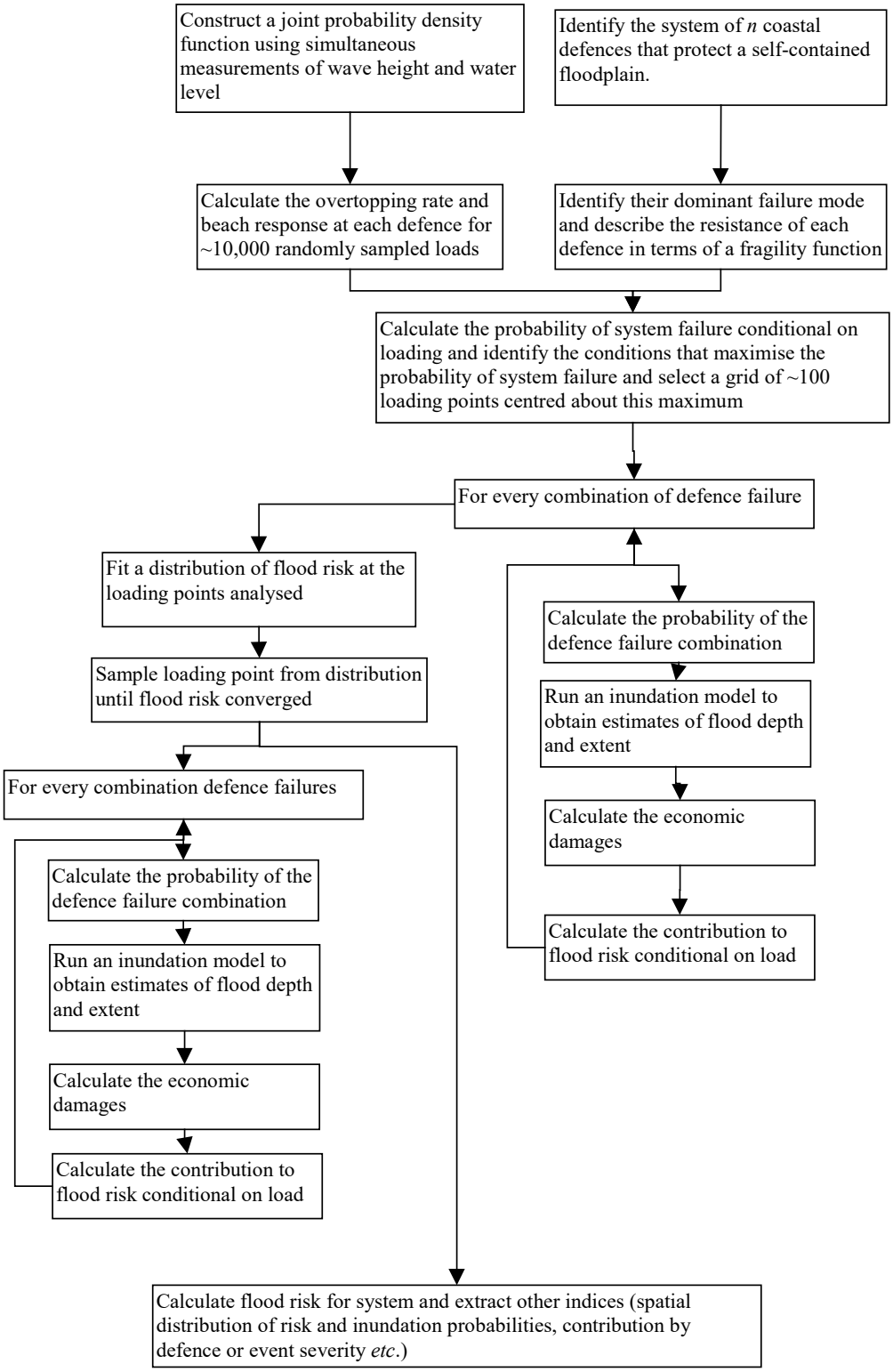

Figure 2.1 Overview of risk-based importance sampling methodology

2.1 Flood defence systems reliability analysis

For a given defence system, the separate defence sections are assumed to have independent and usually different resistances to flood loading. Failure of one or more of the defences by overtopping or breaching will inundate a part of, but not necessarily all, of the floodplain. The probability of every combination of defence failure that may cause flooding in the floodplain is required. Consider a flood defence system with n defence sections, labelled d_1, d_2,…, d_n the failure of defence d_i is labelled as D_i and non-failure as $\overline{D_i}$. There are 2^n system states whose probabilities are to be estimated. For a large system, the analysis of all possible system states requires excessive computer processing time.

Computing resources are further burdened by the need to consider joint loads on coastal defences. In the fluvial situation the 1 in 100 year event refers only to one extreme water level, whereas for coastal defences, the same return period refers to a set of combinations of water levels and wave heights. The nature of loading for an event of a given return period will influence both the probability of failure of the defence system and the consequences of failure. Whereas a large wave height and low water level event will result in a greater chance of defence breaching, a lower wave height combined with a higher water level will result in greater inundation should a breach occur. In order to calculate the contribution of the 1 in 100 year event towards the total flood risk it is therefore necessary to analyse a number of events.

Clearly the computational time to analyse 2^n defence failure combinations for each combination of wave height and water level is excessive. An efficient risk-based importance sampling routine has therefore been developed. The approach is described in the following sections.

Fragility

The resistance of each defence i (i = 1,…, n) in the system is described in terms of a fragility function, conditional upon loading. The fragility, as defined by Casciati and Faravelli (1991), of a structure is the probability of failure, conditional on a specific loading, l. If the failure of a structure is described by a limit state function Z such that $Z \leq 0$ represents system failure and $Z > 0$ represents the not failed condition, then the fragility function $F(l) = P(Z \leq 0 \mid l)$. A fragility curve (Figure 2.2) is a plot of the conditional probability of failure of a dyke revetment given varying loadings. Thus in general the fragility will be a function of several loading variables $l_1 \ldots l_n$. The failure probability of a defence, $P(D)$, can be established by integrating the fragility curve over the loading distributions.

$$P(D) = \int_0^\infty p(l_1 \ldots l_n) P(D \mid l_1 \ldots l_n)\, dl_1 \ldots dl_n \qquad (4)$$

where $p(l_1 \ldots l_n)$ describes the loading space for one or more loading variables and $P(D|l_1 \ldots l_n)$ is the fragility curve conditional on the loading(s). For a coastal defence, the loading is likely to be overtopping rate Q_i: $F(D_i|Q_i)$, or wave height H_{si}: $F(D_i|H_{si})$, water level W_i: $F(D_i|W_i)$ or a combination of the two: $F(D_i|H_{si},W_i)$ where D_i denotes failure of defence i (Dawson and Hall, 2003*a*, 2003*b*).

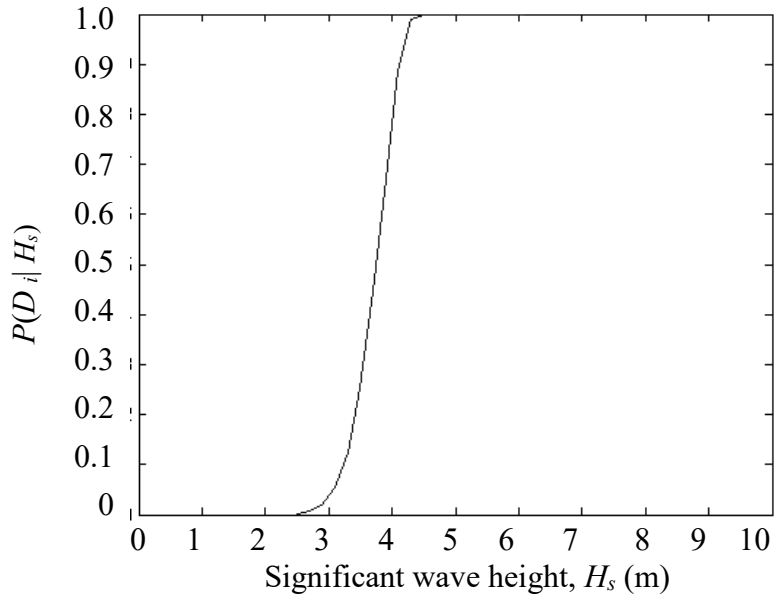

Figure 2.2 A fragility curve that establishes the relationship between wave height and defence failure probability

2.1.1 Statistical estimation of extreme loads

A joint probability density function $f(H_s, W)$ is constructed using simultaneous measurements of wave height H_s and water level W at the site. In order to estimate the probabilities of extreme combinations of wave height and water level, the joint density approach of Hawkes *et al*. (2002) is used. The method is described fully by Hawkes *et al*. (2002) and HR Wallingford and Lancaster University (2000), but the salient points are reproduced here.

1. The input data are prepared; each record consists of a simultaneous record of wave height, H_s, wave period, T_m, and water level, W, at a given location. Each high water is extracted and taken to be an independent record.

2. Statistical distributions are fitted to H_s, W and wave steepness, γ, (this is a more robust variable than T_m for statistical calculations). Commonly occurring conditions are well represented within the record and below a user-defined threshold (for H_s, W and γ) the distributions are represented empirically by the observed values. Above the threshold (*ie*. for extreme values) the Generalised Pareto Distribution (GPD) is used:

   $$\text{GPD}(\sigma,\xi): P(X \leq x | X > u) = 1 - \{1 + \xi(x-u)/\sigma\}^{1/\xi} \quad (1)$$

   This defines the cumulative probability distribution (c.p.d.) of variable X, given X is greater than the user-defined threshold u, where $\sigma(\sigma>0)$ is a scale parameter and ξ is a shape parameter. Whilst the GPD is invariant of the threshold level, the level must be selected with care; too high a threshold and there are insufficient exceedances to estimate the GPD parameters accurately and too low a threshold and the asymptotic justification for the GPD will not hold. The mean residual life plot (Davison and Smith, 1990) is often used to support the selection of this level.

3. A dependence function is fitted to the wave height and water level data. Distributions of H_s and W are transformed to standard Normal distributions, N~(0,1). A correlation coefficient, ρ, is calculated from the bivariate normal distribution that defines the relationship between the two parameters. A Bivariate normal distribution is used as its dependence characteristics are well understood.

4. Thousands of years of sea conditions are simulated, capturing extreme values and variable dependency for H_s, W and γ (which can be transformed back to T_m). Combinations of H_s and W below the threshold are sampled from the population distributions whilst values exceeding this threshold are sampled from the bivariate normal distributions.

Below the threshold level set in Step 2, the Monte Carlo simulation can only select from amongst the discrete values existing in the original data sets, resulting in a 'striping' effect (this can be seen in the data used for the example application in Figure 3.2). Where loading conditions vary within the defence system (for example, either side of a headland) this process should be repeated for each set of conditions. The corresponding loading distribution is used to estimate defence failure probabilities.

2.1.2 Response functions

A random sample of a large number (~10,000) of points from the j.p.d.f. $f(H_s, W)$ are taken. For each point in this sample the cross shore response at each defence $i = 1,\ldots, n$ in the system is calculated. This response is in terms of the overtopping rate, $Q_i(H_s, W)$, and the output from a structural response function selected to reflect the likely failure mode of the defence section. Since parametric calculations are computationally inexpensive, no importance sampling is required at this stage.

The Overtopping Manual (HR Wallingford, 1999) is used to calculate the overtopping volume for each defence section. The manual lists functions to define the overtopping discharges for sea walls depending on their roughness, permeability, slope and whether they have a berm or crown wall.

An appropriate response function is selected for each defence, based on its type, condition and the width and volatility of the foreshore. For example, an expert may identify a particular dyke that is protected by a rock revetment as being most likely to fail through loss or damage to its armour stone. Either Hudson's equation (USACE, 2002), or Van der Meer's equations (Van der Meer, 1988) may be used to assess stability under particular loading conditions. A full review of failure mechanisms is beyond the scope of this paper which considers only those relevant to the example implementations. A number of publications provide a substantial review of these functions, including (but not exclusively) CIRIA and CUR (1991), CIRIA (1996), USACE (2002) and Dawson (2003).

2.1.3 Sampling methodology

The probability of failure, $P(D_i)$, for each defence for each sample of (H_s, W) is estimated from the fragility curves using Equation 1. The conditional probability of *system* failure, $P(D_s|H_s, W)$, for each of these samples is calculated assuming independence between defence sections:

$$P(D_s \mid H_s, WL) = \prod_{i=1}^{n} \left[1 - P\left(D_i \mid H_{si}, W_i\right)\right] \quad (1)$$

The distribution of conditional flood risk is unknown, so an initial sample of m points ($m \cong 100$) is selected. Because flood risk is a function of probability, these points are positioned on a regular grid centred on the point t on $H_s \times W$ that maximises $P(D_s|H_s, W).f(H_s, W)$. This point does not necessarily correspond to the maximum on the distribution of flood risk.

As described previously, for each point $j = 1,\ldots, m$ there are 2^n possible defence failure combinations. For each of these, the conditional probability $P(D_k|H_s, W)$, $k = 1,\ldots, 2^n$ is calculated (again, these calculations are computationally inexpensive). The r failure combinations that make a non-negligible contribution to the total conditional probability of system failure $P(D_s|H_s, W)$ (generally $r <<< 2^n$) are selected.

For each failure combination $k = 1,\ldots, r$ the inundation model is run using the loading conditions (H_s, W), the overtopping rates $Q_i(H_s, W)$ as boundary conditions and an empirical estimate of the breach size and discharge, for breaching failure modes. The risk-based sampling methodology is independent of the inundation modelling. A summary of the inundation model used in the example implementation is provided later in this paper.

For each run $k = 1,\ldots, r$ of the inundation model the economic damage E_k is estimated. A national database (known as AddressPoint) provides information on property type and location in England and Wales. For each property type, Penning-Rowsell *et al.* (2003) have defined a depth-damage relationship (Figure 2.3).

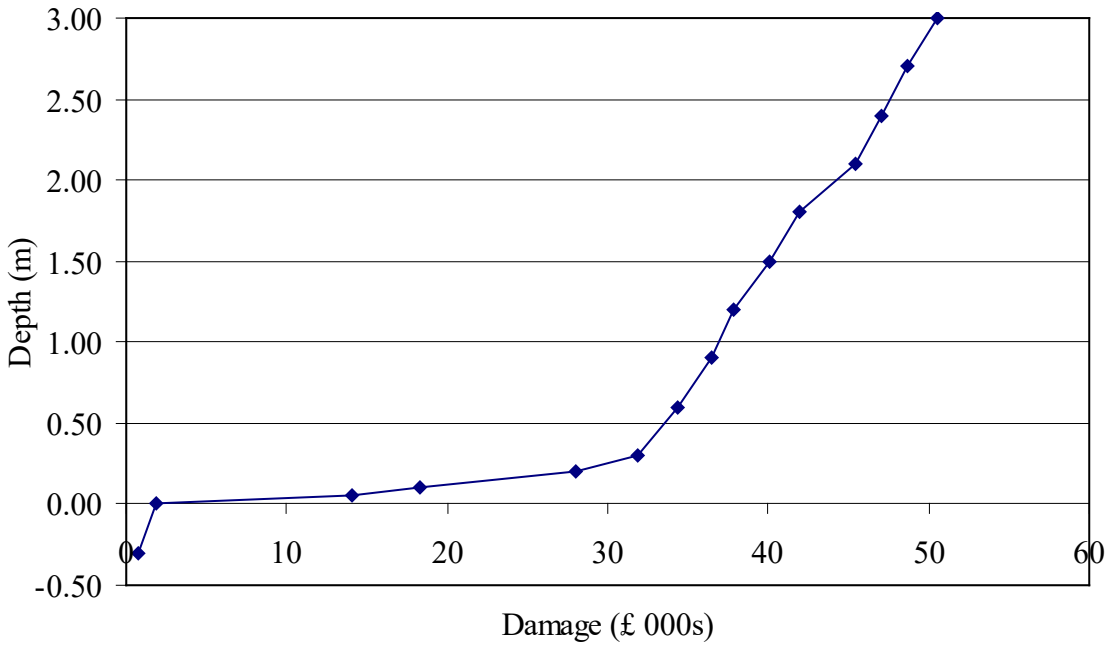

Figure 2.3 Depth-damage curve of a residential property flooded for longer than 12 hours (Penning-Rowsell *et al.*, 2003)

The conditional risk $R(H_s, W)$ for a given combination of H_s and W is calculated by summing the individual contributions from each of the defence failure combinations:

$$R(H_s,W)=\sum_{k=1}^{r}P(D_k \mid H_s,W).E_k \tag{2}$$

The quantity $f(H_s, W).R(H_s, W)$ for each point $k = 1,\ldots, r$ is plotted on $H_s \times W$. These points are used to estimate the risk-based importance sampling distribution by fitting a j.p.d.f., $f_{imp}(H_s, W)$. A point (H_s,W) is sampled from this distribution and using the steps outlined above its conditional risk is calculated. The distribution of conditional risk $R_{imp}(H_s,W)$ is then updated. This is repeated until the conditional risk has stabilised satisfactorily. The total flood risk R_{tot} is given by:

$$R_{tot}=\iint R_{imp}(H_s,W)f(H_s,W)dH_s dW \tag{3}$$

which may be obtained by numerically integrating $R_{imp}(H_s,W)$ with the j.p.d.f. $f(H_s, W)$.

2.2 Inundation modelling

Inundation resulting from a storm surge is driven by a number of physical processes, including gravitational forcing, variations in density, currents and wind stress (Pugh, 1987). Numerical models of such flows range in complexity from fully three-dimensional solutions of the Navier-Stokes equations (Cugier and Le Hir, 2002) to models that treat flow as one-dimensional across a flow path in the floodplain. Simulation of inundation over low-gradient tidal floodplains with significant flood defence structures requires at least a two-dimensional modelling approach with relatively high spatial resolution to represent the complex geometry of the floodplain. However, full two or three-dimensional modelling remains computationally prohibitive on a broad scale, particularly if multiple scenarios are to be modelled.

The risk assessment methodology is not dependent on the use of a particular inundation model, the only requirement being that it can produce a spatial distribution of flood depths within the floodplain. However, to reduce the computational burden of the hydrodynamic calculations for this study a simple 2-D raster based inundation model called LISFLOOD-FP was selected (Bates and De Roo, 2000). This model is quasi-2D in that the flood wave propagation is represented as an approximation to a 2D diffusive wave. The floodplain is discretised as a grid of rectangular cells. Flow between cells is calculated simply (Figure 2.4) as a function of the free surface height difference across each cell face:

$$Q=\frac{h^{5/3}}{n}\left(\frac{h^{i-1,j}-h^{i,j}}{\Delta x}\right)^{1/2}\Delta y \tag{5}$$

Change in water depth in a cell over time t is then calculated by summing the fluxes over the four cell faces.

$$\frac{dh^{i,j}}{dt}=\frac{Q_x^{i-1,j}-Q_x^{i,j}+Q_y^{i,j-1}-Q_y^{i,j}}{\Delta x\Delta y} \tag{6}$$

where $h^{i,j}$ is the water free surface height in cell (i,j), Δx and Δy are the cell dimensions, n is a friction coefficient, and Q_x and Q_y describe the volumetric flow rates between

floodplain cells. Equations 4 and 5 give similar results to a more accurate finite difference discretisation of the diffusive wave equation but with much reduced computational cost, and have been shown to perform as well as full two-dimensional codes (Horrit and Bates, 2001).

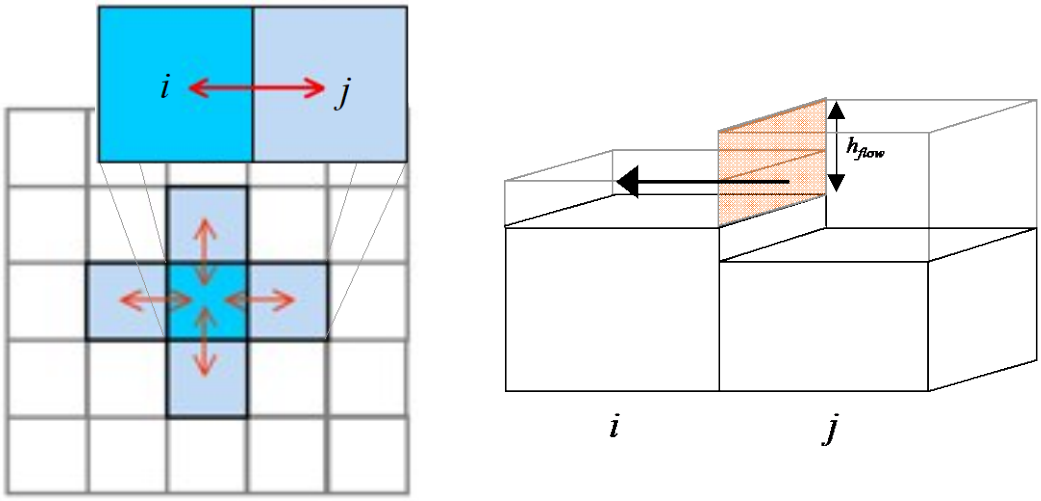

Figure 2.4 Representation of flow between floodplain cells

3. EXAMPLE IMPLEMENTATION OF THE ILM AT A COASTAL SITE

3.1 Background to Towyn

The case study site selected is Towyn in North Wales (Figure 3.1b). Towyn is situated on the estuary of the river Clwyd and is built on large areas of coastal lowland that were reclaimed during the 18th century. A large proportion of the inhabitants live in caravans and are elderly and therefore particularly vulnerable to flooding.

Towyn was inundated in February 1990 when 467m of seawall was breached by a severe storm event when a 1.3m storm surge at high water coincided with 4.5m high waves. A lack of natural protection meant that the seawall, which had been targeted for maintenance in the near future, felt the full force of the waves. The nature of the topography resulted in the flood reaching as far as 2km inland with a maximum depth of 1.8m (Roe, 1993). Although there were no direct fatalities, 5000 people had to be evacuated from nearly 3000 properties. The total cost of the flood was estimated as being in excess of £50million (HR Wallingford, 2003).

The areas of Indicative Flood Plain within the Pensarn to Kimnel Bay flood plain (referred to as Towyn) are now defended by extensive coastal defences. It is particularly relevant to note that some of the defence lengths have been reconstructed in the past 10-12 years, with associated improvements being provided in the Standard of Protection. For example, across the Pensarn frontage rear flood walls have been constructed along the crest of the shingle bank, whilst the Towyn section received extensive armour stone revetments, following breaching of the defences and hinterland flooding as a result of the February 1990 storms. Also in the late 1990's improvement works to the sea wall were carried out across the Kinmel Bay frontage.

Along significant lengths the beach plays an important part in providing primary defence. Robust flood risk assessment will need to recognise the level of service that this provides and identify those sections that are most vulnerable to future breaching.

The Indicative Flood Plain Map provided by the Environment Agency is developed from a projection of the 200-year return period water level and ignores the presence of defences. Therefore it is reasonable to assume that the estimate of flood extent in such an event is overestimated by the IFM.

The area identified for examination in the study is situated between Pensarn and Kinmel Bay (see Figure 3.1a and 3.1b)

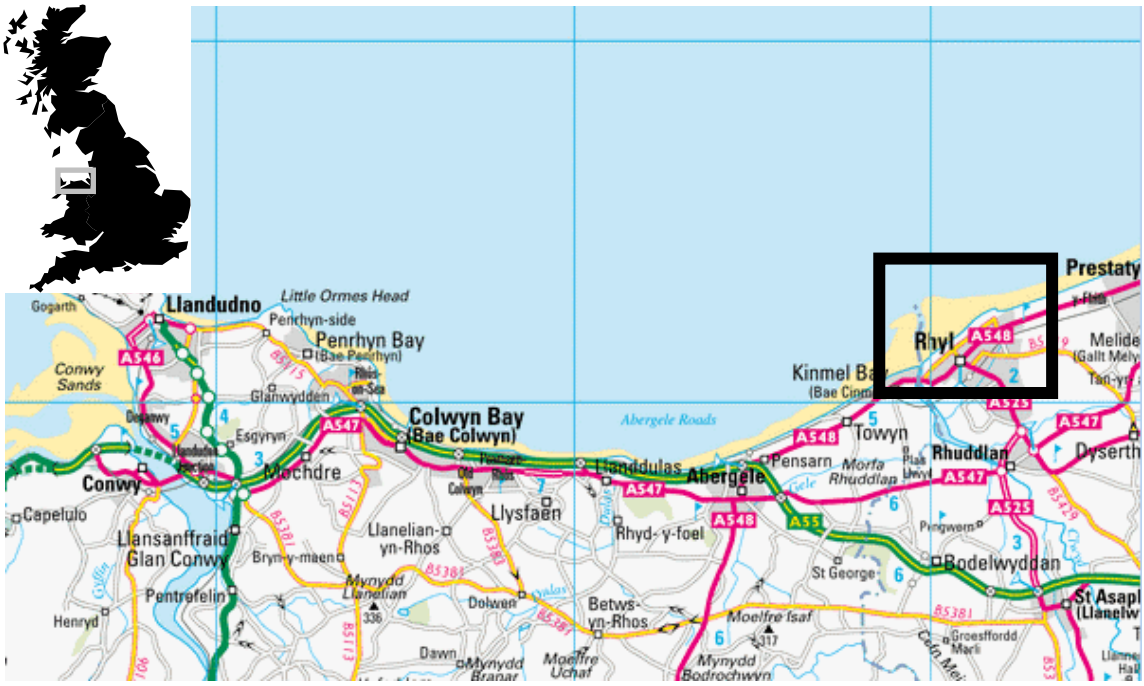

Figure 3.1a Location map

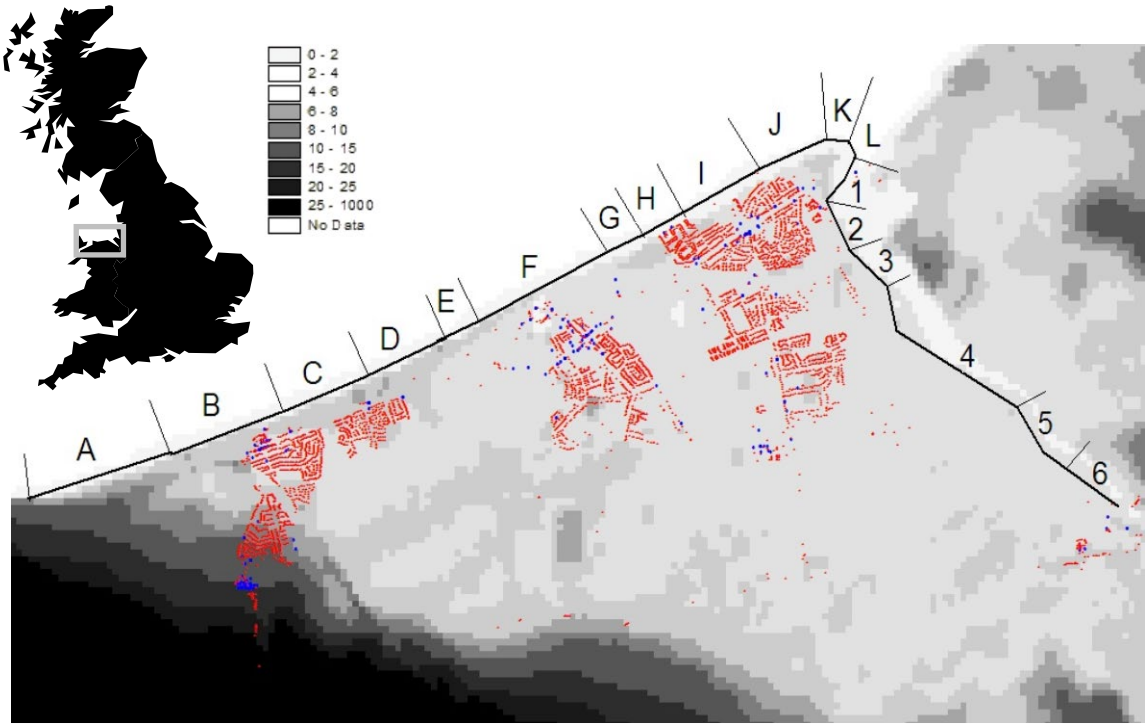

Figure 3.1b The Towyn floodplain (darker shades represent higher ground measured in mAOD) showing the location of residential and non-residential (darker points) property and the defence sections

3.2 Examination of historical flooding

3.2.1 Introduction

Significant flood events have occurred in the past relating to the area under examination, most significantly when the British Rail defences at Towyn were breached in 1990, which lead to extensive hinterland flooding and damage estimated to be in excess of £50 million.

The database of reports relating to coastal defence and flooding issues was examined together with other sources to identify dates of known past flood events. In addition, archives of local newspapers were also accessed to identify any articles and press coverage relating to these events.

Based on the review of historical data on flooding, thirty records of past flooding have been identified. These range from minor tidal incursions through to more significant and extensive breaching of the coastal defences and subsequent widespread inundation (for example the events of 26-28 February 1990 when high tides and winds caused overtopping and a 467m long breach in the seawall.)

The details of the information collated on historical flooding are recorded in Appendix 3 under the following headings:

- Event date
- Area affected
- Event details
- Hinterland consequences – where known
- Further comments
- Source of information

3.2.2 Review of sea conditions during the historic events

The historical event data were compared against the analysis of present day extreme wave and water levels. This comparison provides an interesting insight into the return period of past events and the degree to which the recent climate is similar to that experienced in the past. To aid this comparison, key tidal flood events identified above that have an associated quantifiable water level or wave height have been reviewed in light of the analysis of extremes and assigned an appropriate return period for general interest.

Events prior to 1970

Three 'events' between 1899 and 1924 are said to have involved a predicted tide of 30-31 feet at Holyhead. Presumably this is to an older unknown datum, as HAT at Holyhead is only 20.7 feet above Chart Datum. On two of these three occasions a surge of 3.35 feet was noted, which has a return period of around 5 years. One entry for 1937 notes a surge of 1.5 feet at Holyhead that would have a return period of about 0.02 year.

Measured sea level and modelled wave conditions are available from 1970 onwards, in a form suitable for direct comparison with sea conditions used in this study.

11/12 Feb 1990
Precise times and measurements are not available for this event, but the sea level had previously been shown to have a return period of about 1.5 years, and the predicted H_s was about 3.5m throughout 12/Feb (about 10 years joint return period).

26-28 Feb 1990 (Towyn breach event)
There were five successive high waters, each of which might have been considered an 'event' in its own right. The two highest records were at:

- 12.00/26/Feb, 11.06mCD at Liverpool (about 80 years return period based on data prior to that occurrence, and 30 years when Feb 1990 included) with an H_s of 4.32m (about 1.5 year return period for wave height; 500 years joint exceedance return period based on data prior to that occurrence, and 100 years when Feb 1990 included), and

- 11.00/27/Feb, 10.82mCD at Liverpool (about 7 years return period) with an H_s of 4.22m (about 1.2 year return period for wave height; 100 years joint exceedance return period based on data prior to that occurrence, and 25 years when Feb 1990 included).

(The recorded water level at Deganwy Dock of 5.15mOD suggests about a 7 year return period sea level when Feb 1990 data is included.)

Conclusions from the historic event analysis

It is interesting to note that most of the marine flooding events were caused by extreme sea levels coupled with high wave conditions. This indicates that the worst marine flooding is driven primarily by very high sea levels, sometimes persisting over a number of successive high waters, but that high wave conditions at the same time are also a contributory factor.

3.3 Inspection of existing data

In this task, the basic information relating to the database of coastal defence structures was reviewed through comparison with existing as-built drawings and by visual inspection. In particular, an assessment was made of the geometry and condition of the defences.

Data was collected from different sources to inspect and confirm the adequacy of the data held by CBCC Engineering and Environmental Services including:

- Eighty-nine past reports
- Foreshore and bathymetric surveys
- Hinterland topography data
- Flood plain and OS mapping data
- Photographic records of coastal development and past failures
- Defence details – as-built drawings, past surveys and existing databases
- Environmental data on waves and water levels.

The data collated and reviewed under these headings are listed in full in Appendix 1.

This existing was then supplemented by data gathered through a 'walk-over' survey of all defences. In particular the survey focused on a number of aspects:

- Establishing a local defence coding linked to NFCDD and past CBCC studies
- Defence location (OS grid refs)
- Defence length
- Description of the primary, secondary and tertiary defence details (i.e shingle beach, backed by a secondary sea wall etc)
- Beach gradient
- Levels (mOD) of primary, secondary and tertiary defence crests
- Year of construction(s) if known
- Condition of primary, secondary and tertiary defences
- Comments on likely defence performance and other general issues
- Profile and cross-section
- Details of on-going monitoring
- Maintenance responsibilities
- NFCDD cross reference
- References to photographic records.

The details of the revised database are presented in Appendix 2.

In addition to the above, cause-consequence diagrams have been produced (See Appendix 5) for each of the defence lengths identified. Each diagram outlines the:

- Sources of risk
- Risk pathways
- Risk receptors
- And the potential harm that be experienced in the event of a flood.

Based on this analysis a dominant failure mode has been identified for each defence. This dominant failure mode is later used in the construction of the defence specific fragility surfaces.

3.4 Marginal wave and water level conditions

Extreme waves and extreme water levels have been estimated for several locations between Llandudno and Rhyl for a range of return periods up to one thousand years. In view of the large number of previous studies in the area, the approach adopted was not to do any new modelling of sea conditions, but to develop all necessary results by re-interpretation of existing results and reports.

The widely quoted HR Wallingford Report EX2133 on extreme waves and water levels for the North Wales coast (HR Wallingford, 1990) was taken as the starting point. This was supplemented by more recent extreme water levels predictions based on research at the Proudman Oceanography Laboratory (POL, 1997) to provide extreme water levels for the study area. Offshore wave conditions predicted within EX2133 have not been revised. However, they have been transferred nearshore using site-specific wave transformation functions to provide nearshore wave climates at a series of points. The

analysis of joint exceedance within EX2133 has also been extended to include return periods of combinations of wave and water levels up to 1000 years.

3.4.1 Dependence between large offshore waves and high water levels

The main results of EX 2133 are expressed in terms of the probability of joint occurrence of large waves (offshore Rhyl) and high water levels (at Liverpool) for joint return periods between 1 and 100 years. The dependence between large waves and high water levels is higher than the UK average. Results compared well with a later analysis of the same data set using a different analysis technique (HR Wallingford with Lancaster University, 2000). Hence, they have not been updated for the present study.

3.4.2 Nearshore sea conditions

The extreme deep water sea conditions discussed above were transformed inshore as follows:

- Individual sea levels (at Liverpool) were replaced by site-specific sea levels with the same return periods.

- Individual significant wave heights were replaced by the site-specific wave heights with the same return periods.

- Wave periods were reproduced unchanged from offshore.

Note: ***Influence of local wave breaking*** All significant wave heights used are *unbroken* (since allowance for breaking is specific to the exact location and sea level being used). Wave breaking has therefore been taken account of in the overtopping and other defence response models used later in this report. However, for guidance, and for use outside of a coastal response model that includes the influence of breaking, the significant wave heights quoted above should be reduced to about 60% of the local water depth (e.g. at the toe of a structure) to allow for local depth-limitation of wave height.

3.4.3 Nearshore sea levels

Nearshore extreme sea levels were taken from predictions in POL (1997).

3.5 Joint loading conditions and waves and water levels

Using the joint probability method described earlier in this paper, 10,000 years of joint events were generated. A plot of all the joint events and the resulting j.p.d.f. are shown in Figure 3.2 and Figure 3.3.

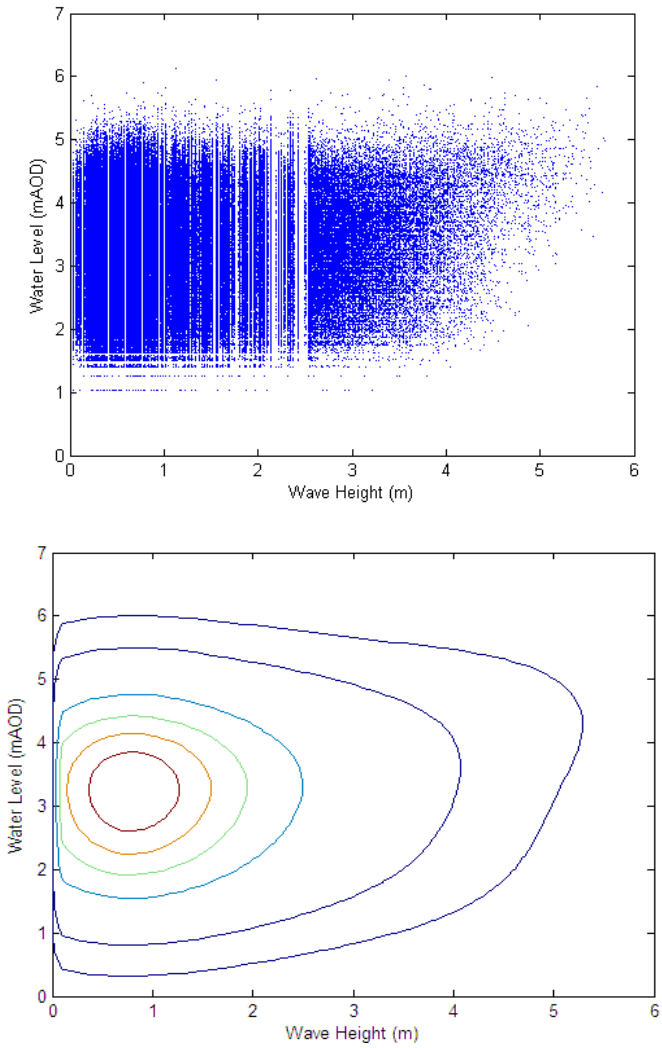

Figure 3.2 The output of the joint probability simulation
(refer to the earlier section on joint probability estimation for explanation of the 'striping') and contours of the j.p.d.f. (at $f(H_s,W)$=0.2, 0.15, 0.1, 0.05, 5×10^{-3} and 5×10^{-4}) after the population is smoothed using kernel density estimation methods.

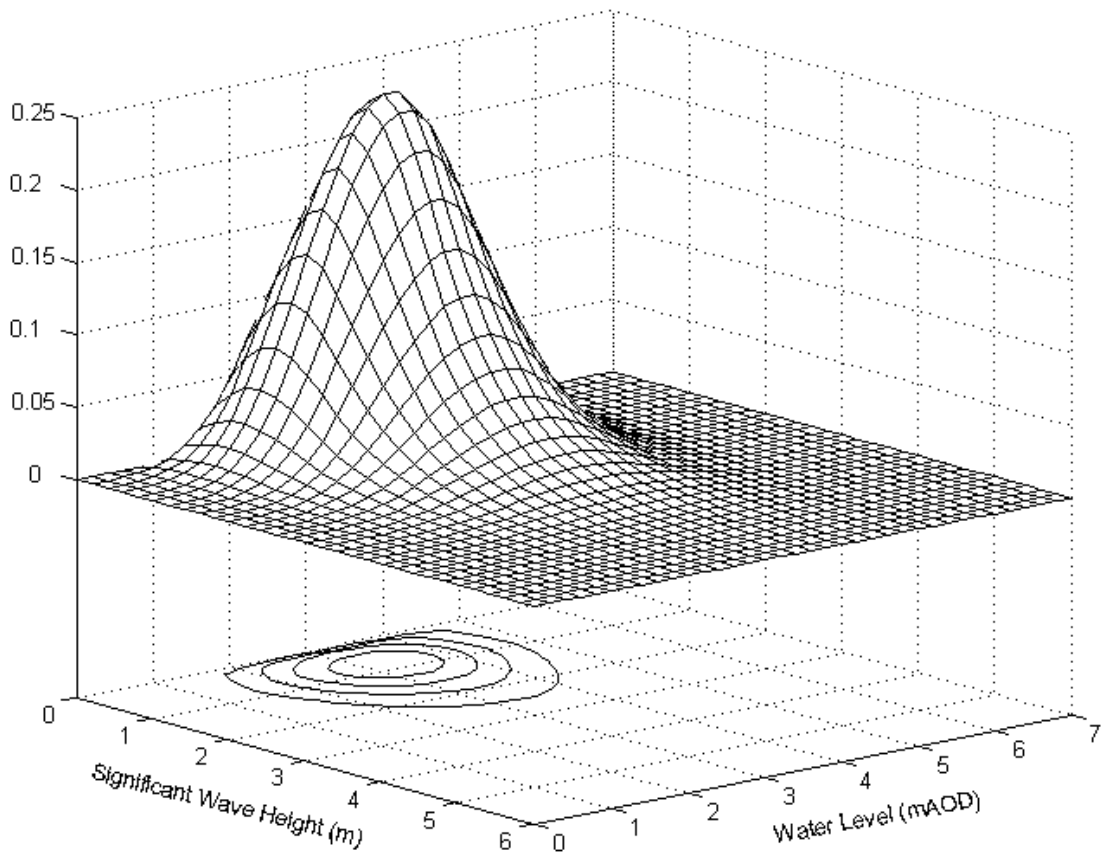

Figure 3.3 Joint probability density plot of water level and wave height

3.6 Summary of the defence system

HR Wallingford (1985) indicated that water levels in the estuary are controlled by sea level alone, and the influence of waves and river flows in the estuary can be ignored. On the open coast waves and water levels are important. The estuarial defences are not prone to overtopping even during extreme events, although they may be breached.

The defence system comprises of 14 coastal defence sections (labelled A-N, where defence F was breached during the 1990 floods) and six fluvial defence sections (labelled 1-6). These are currently all protected by a shingle beach that is recharged in places. The defences vary along the coastline with crest heights ranging from 7m AOD to over 9m AOD.

Table 3.1 Description and likely dominant failure mode for each defence section (locations shown on Figure 3.1b)

Defence section	Defence information	Dominant failure mode
A	Shingle bank with rear vertical wall	Shingle beach erosion
B	Shingle bank with rear vertical wall	Shingle beach erosion
C	Sloping concrete revetment with crown wall	Overtopping damage
D	Sloping armour stone revetment	Rock armour damage
E	Shingle bank with grouted block revetment and crown wall	Shingle beach erosion
F	Sloping armour stone revetment	Rock armour damage
G	Sloping armour stone revetment	Rock armour damage
H	Shingle bank with sloping armour stone revetment and rear vertical wall	Shingle beach erosion
I	Shingle bank with rear vertical wall	Shingle beach erosion
J	Sloping armour stone revetment with rear vertical wall	Rock armour damage
K	Dunes	Dune erosion
L	Dunes	Dune erosion
M	High ground	n/a
N	High ground	n/a
1	High ground	n/a
2	High ground	n/a
3	High ground	n/a
4	Earth embankment	Piping
5	High ground	n/a
6	Earth embankment	Piping

3.7 Defence failure modes and defence fragility

Two primary failure modes have been considered:

- Overtopping (non-structural failure);
- Breaching (structural failure).

The analysis of both of these failure modes is discussed below together with results.

3.7.1 Defence overtopping

Overtopping is an exponential function derived empirically that varies depending on the geometry, permeability and roughness of the structure. For an impermeable, sloped seawall, the mean overtopping discharge per metre run, Q, is given by (HR Wallingford, 1999):

$$Q = A T_m \, g \, H_s \, e^{-\left(B \, Rc / Tm \left(g \, Hs^{0.5} \right) \right) / r} \qquad (3)$$

where g is the gravitational constant, A and B are empirical coefficients dependent on the cross section of the seawall, r is a roughness coefficient (with a maximum value of 1 representing a smooth wall), T_m is the mean wave period at the toe of the seawall, H_s is the significant wave height at the toe of the seawall and R_c is the freeboard (the height of the crest above still water level). The Overtopping Manual (HR Wallingford, 1999) provides further detail on the necessary adjustments for other sea wall configurations.

Using the above methodology, for each defence length identified, an upper and lower bound estimate of overtopping discharge has been predicted for a range of return period events. The upper estimates were calculated using the lowest defence crest level. The lower estimates were calculated using the highest defence crest level. In both cases the same prediction of the extreme water levels was taken. This means that for each load scenario an estimate of the overtopping volume is deterministically calculated. The overtopping volumes were calculated for all defences as boundary conditions for the hydrodynamic model. This is in contrast to the HLM where a probabilistic approach to the calculation of overtopping was necessarily adopted.

3.7.2 Defence breaching – Probability of occurrence

With regard to more catastrophic failure modes, breach probabilities are difficult to predict. Predicting breach growth and maximum size is equally problematic and at present beyond the capabilities of existing numerical tools. However, breach events represent the most significant of flood scenarios and are of considerable importance in determining flood risk.

In considering the likelihood of breach, the critical failure modes outlined in the cause-consequence diagrams and summarised in Table 3.1 have been analysed as an indicator of the probability of breaching. The following criteria have been used to determine the likelihood of failure associated with each dominant failure mode. The method of analysis for each of the dominant (breach) failure modes are discussed below.

Overtopping (leading to a breach)
Damage caused by overtopping water to the promenade or the rear of the structure can lead to a breach in the defence. The overtopping spreadsheet was used to estimate the overtopping rates for each defence then the following criteria were used to compute the probability of breaching (HR Wallingford, 1999) for both embankments and revetments as described in Tables 3.2 and 3.3 below.

Table 3.2 Probability of breaching in the event of embankment overtopping

Overtopping Rate, Q (m^3/s)	Breach probability, p	
	Upper Bound	Lower Bound
0.0001	0.0	0.0
0.0020	0.1	0.0
0.0500	0.2	0.1
0.5000	0.3	0.2
5000.0	1.0	0.3
500000.0	1.0	1.0

Table 3.3 Probability of breaching. Revetment Overtopping

Overtopping Rate, Q (m^3/s)	Breach probability, p	
	Upper Bound	Lower Bound
0.0050	0.0	0.0
0.0500	0.1	0.0
0.2000	0.2	0.1
2.0000	0.3	0.2
7000.0	1.0	0.3
70000.0	1.0	1.0

Rock armour damage

Failure due to rock armour damage uses Van der Meer's stability formulae:

$$H_s = 6.2 S_d^{0.2} P^{0.18} \Delta D_{n50} (\cot\alpha)^{0.5} s_m^{0.25} N^{-0.1} \quad (1)$$

for plunging waves, and

$$H_s = S_d^{0.2} P^{-0.13} \Delta D_{n50} (\cot\alpha)^{(0.5-P)} s_m^{-0.5P} N^{-0.1} \quad (2)$$

for surging waves, where S_d is the damage number; P is the permeability factor; $\Delta=\rho_{rock}/\rho_{water}-1$; D_{n50} is the nominal rock diameter; α is the revetment slope; s_m is the mean wave steepness; N is the number of waves attacking the structure.

Van der Meer's equation enables the likely degree of damage to be calculated through the stability parameter(S_d). S_d has been related to the probability of failure (p) as shown in Tables 3.4 and 3.5:

Table 3.4 Probability of Breaching. Damage to rock armour. Defence Lengths 4D & 4F

Stability Number, S_d	Breach probability, p	
	Upper Bound	Lower Bound
0.0	0.0	0.0
1.0	0.05	0.0
1.5	0.3	0.05
5.0	1.0	0.3
10.0	1.0	1.0

Table 3.5 Probability of Breaching. Damage to rock armour. Defence Length 4G

Stability Number, S_d	Breach probability, p	
	Upper Bound	Lower Bound
2.0	0.0	0.0
2.5	0.15	0.0
3.0	0.3	0.15
5.0	1.0	0.3
10.0	1.0	1.0

Table 3.6 Probability of Breaching. Damage to rock armour. Defence Lengths 4J

Stability Number, S_d	Breach probability, p	
	Upper Bound	Lower Bound
1.0	0.0	0.0
1.5	0.15	0.0
2.0	0.3	0.15
4.0	1.0	0.3
10.0	1.0	1.0

Piping failure

The pressure head difference across a flood embankment can lead to piping (ie water moves freely through the body of the defence) and finally breaching of the whole embankment (Mohamed, 2002). This process is quite complex and is still an active area of research. Combined with the lack of detailed data, the following criterion has therefore been used to quantify the effect of piping (Terzaghi et al, 1996):

$$C_w = \frac{B/3 + \sum t}{H} \tag{10}$$

where C_w is the weighted creep ratio which is based on the type of embankment material, B the width of the structure, t the depth of impervious layers below the embankment and H is the pressure head difference across the embankment.

The Terzaghi formulae has been applied using the values listed in the table below, which give the minimum values of C_w

Table 3.7 Critical values of C_w (Terzaghi et al, 1996)

Embankment Material	Critical C_w (C_{wr})
Very fine Sand or Silt	8.5
Fine Sand	7
Medium Sand	6
Coarse Sand	5
Fine Gravel	4
Medium Gravel	3.5
Coarse Gravel and cobbles	3
Boulders	2.5

C_w can be related to the probability of failure (p) as follows:

Table 3.8 Probability of Breaching. Piping

Weighted Creep Ratio, C_w	Breach probability, p	
	Upper Bound	Lower Bound
1.40	0.0	0.0
1.25	0.1	0.0
1.10	0.2	0.1
1.00	1.0	0.2
0.90	1.0	1.0

Dune erosion

Dune erosion is modelled using Vellinga's equations (CUR and TAW, 1991). An erosion profile is established based on storm conditions. The volume of dune eroded is assumed to correspond to the difference in volume between the initial beach profile and assumed storm profile (CIRIA, 1996). The post-storm position of the crest and therefore the amount of retreat can therefore be calculated. As with shingle beach erosion there is not in general an algebraic limit state function.

Shingle beach erosion

The shingle beach erosion analysis uses a parametric model developed by Powell (1990, 1993) designed to simulate the behaviour of shingle beaches. A schematised beach profile is described by a number of equations which enable the beach profile, and hence the crest retreat, to be calculated for different combinations of wave height and water level.

Breaching due to the retreat of the beach crest in front of the defence. The HR Wallingford SHINGLE model was used to determine the crest retreat of the beach. The following criteria were then used to estimate the associated probability of breaching:

Table 3.9 Probability of breaching. Crest Retreat

Crest Retreat, CR (%)	Breach probability, p	
	Upper Bound	Lower Bound
-25	0.0	0.0
0	0.05	0.0
50	0.2	0.1
100	0.4	0.2
150	1.0	0.4
250	1.0	1.0

where: CR = Crest retreat as a percentage of the initial crest width.
p = Probability of defence failure and breach

Overturning / Collapse of the structure

Scour at the toe of the structure can undermine its foundation and reduce its factor of safety against overturning and finally lead to its collapse. The HR Wallingford SCOUR model was used to determine the scour depth at the toe of the structure and criteria similar to that used in the crest retreat failure mode was used for this failure mode.

Table 3.10 Probability of breaching. Overturning / Collapse of structure

Scour Depth, S_c (m)	Breach probability, p	
	Upper Bound	Lower Bound
0.0	0.0	0.0
0.5	0.05	0.0
1.0	0.2	0.05
2.0	0.4	0.2
3.0	1.0	0.4
4.0	1.0	1.0

where: S_c = Scour depth.
p = Probability of defence failure and breach

3.7.3 Defence fragility

For each defence, a fragility curve, such as that shown in Figure 3.4, was used to summarise the response function. Figure 3.4 shows the fragility curve for shingle beach erosion, in this case defence strength is a function of the crest retreat.

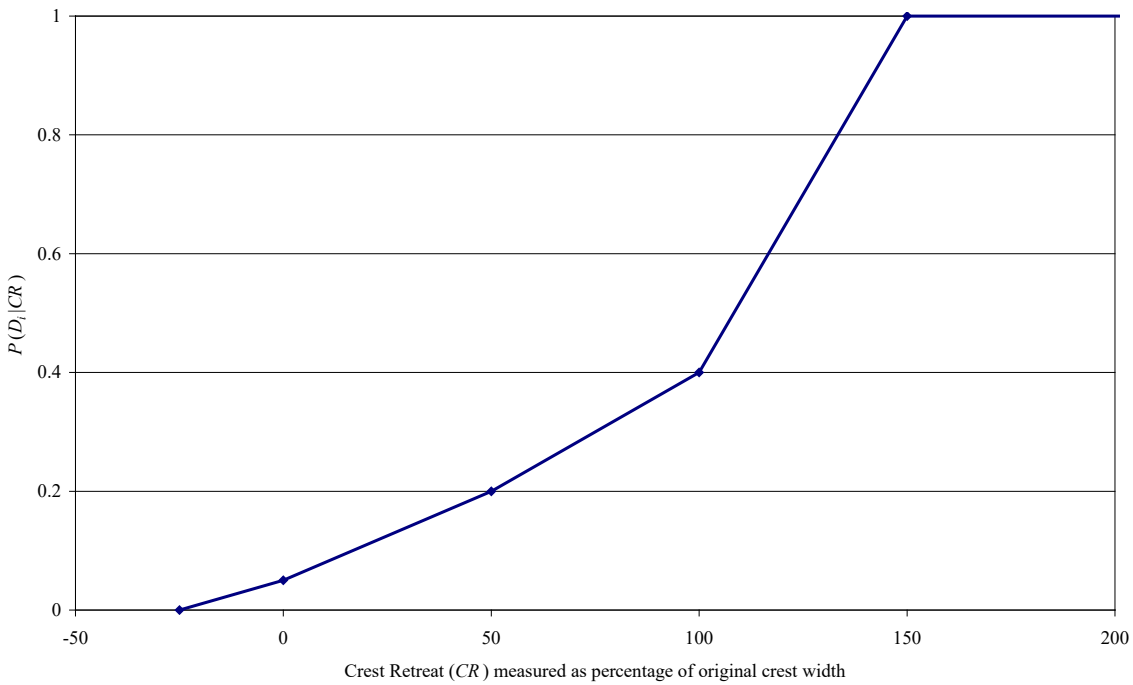

Figure 3.4 Fragility curve for shingle beach erosion

3.7.4 Defence breaching - Breach width and invert

Prediction of breach geometry and growth rate is highly uncertain. A number of breach models have been developed; these are predominantly parametric or physical process based. For even the more sophisticated models currently available, the uncertainty bounds associated with an estimate of the breach width generally have an uncertainty of about +/- 1/3 of an order of magnitude, predictions of failure time have uncertainties approaching 1 order of magnitude and predictions of peak flow between 0.5 and 1 order of magnitude (Wahl, 1998). Many models are time dependent in that they attempt to predict breach growth rates and whilst the risk assessment methodology does not preclude their use, it was considered undesirable to add further computational burden to the inundation modelling process. A simple parametric relationship was therefore adopted in which the breach width and depth were therefore assumed to remain constant for the duration of the flood event. The defence is assumed to breach to the level of the natural terrain. All breaches are assumed to be centred in the middle of the defence.

Research undertaken within the dams sector has produced a number of simplified rules for breach width, including:

$B = h \times a$ (taken from interim results from IMPACT, (HR Wallingford, 2004).

where

a is in the order of 3 for cohesive materials and near 6 for non-cohesive materials.
h = the depth of overflow

Alternatively

$B = h \times 15$ (Visser, 1998)

Within this study therefore breach width has been assumed as a linear function of overflow depth, up to the defence length, relating width to water level as follows:

$$B = \min\{h \times 10,\ L\} \tag{14}$$

where B is the breach width in metres and L is the defence length and h is the water level above the base of the defence.

3.8 Hydrodynamic modelling

Recent flooding provided a means of validating the hydrodynamic model for the site. The hydrodynamic model LISFLOOD-FP, introduced previously, was used to implement the methodology.

The DEM used is predominantly based upon the InterMap SAR data (vertical accuracy of ±1m), but this has been replaced by limited local council manhole survey data (vertical accuracy ±0.05m) where available. The cellsize of the DEM is 50×50m. A boundary condition representing the water level was created along the foreshore and within the river channel. In between this and the floodplain a line of weir cells was defined to represent the defence system. Just behind the defence line, boundary conditions representing overtopping rates were defined. Each storm event analysed was assumed to have a duration of 3 hours.

The model was calibrated using recorded peak wave and water level conditions for the 1990 flood event: W=5.6m, H_s=4.3m. These conditions were used to estimate defence overtopping volumes for this event. Weir cells equivalent to 450m of the defence line were removed to represent the breaching of defence F (Figure 3.5).

Flood depths in Towyn as great as 1.5m were recorded (Roe, 1993). Areas of discrepancy between the recorded and modelled outline most likely result from inaccuracies in the DEM. Whilst some parts of the 1990 flood area are not inundated by the model, others are flooded to depths greater than 1.5m. However, a vertical accuracy of ±1m over most of the survey area and flood depths of similar magnitudes means these discrepancies are not unreasonable. The flood outline itself is predominantly controlled by the land relief. However, two (circled) features on its Southern side are shaped by artificial features; a road and a drainage channel.

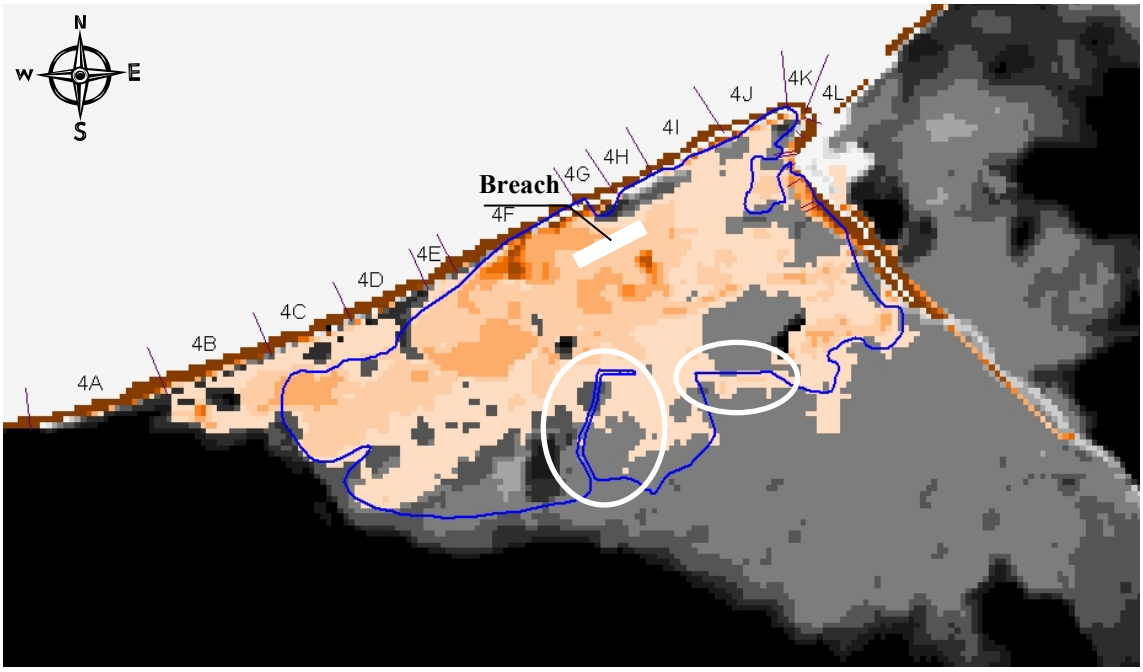

Figure 3.5 The 1990 flood outline superimposed on a model calibration of the same event

3.9 Implementation of risk-based importance sampling routine

The j.p.d.f. of wave height and water level is shown in Figure 3.3. A plot of systems failure probability $f(D_s|H_s,W)$ is shown in Figure 3.6. For lower wave heights, the systems failure probability rises sharply between a water level of 5 and 6m. However, for storm events of large wave height, the rise is less sharp. Figure 3.7 shows the failure surfaces of defences D, K, I and 4. These show the probability of failure conditional on joint loading conditions. It can be seen that these surfaces take different shapes; failure of defence 2 is independent of wave height, whilst the failure of the other defences is controlled by both wave height and water level, with defences D and K forming a concave surface and defence I forming a convex surface. Even under extreme loading it can be seen that defence D is very unlikely to fail whereas defence K has a high failure probability for comparatively low return period events. It is evident that defence 2 dominates the systems failure probability at extreme water levels – especially for low wave height events when failure of other defences is unlikely. However, for W<5.5m and H_s>2m the systems failure probability is dominated by the failure of defence J and K.

Multiplying the systems failure probability distribution and the loading distribution generates the surface plotted in Figure 3.8 as a series of contours; the darker contours represent higher values, whilst three peak values are marked with circles (1 represents the largest peak value, 3 the smallest). A grid (also shown in Figure 3.8), approximately centred on peak 1, was used as the initial sample points for the risk assessment. The initial risk surface generated from these points is shown in Figure 3.9 and gives a total flood risk of £44,000.

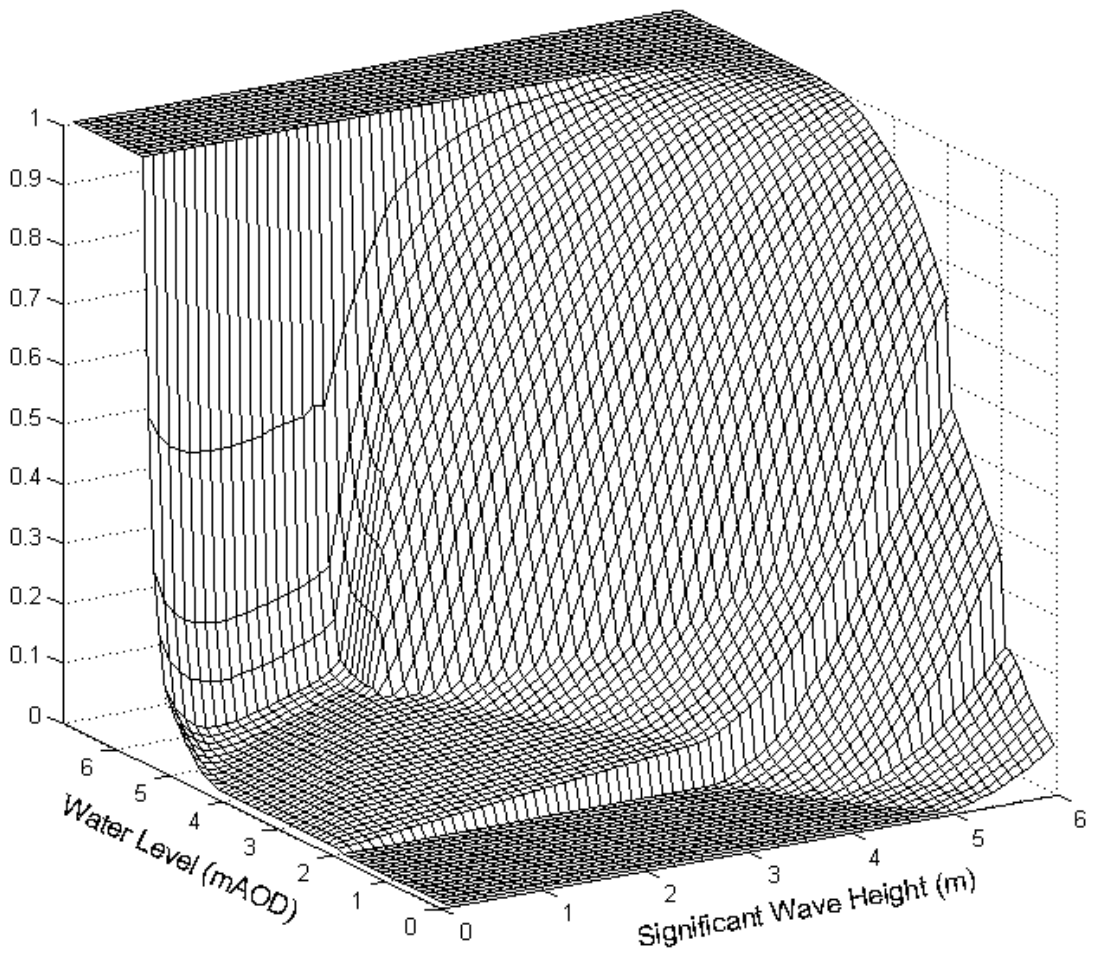

Figure 3.6 Surface describing systems failure probability over a range of loadings

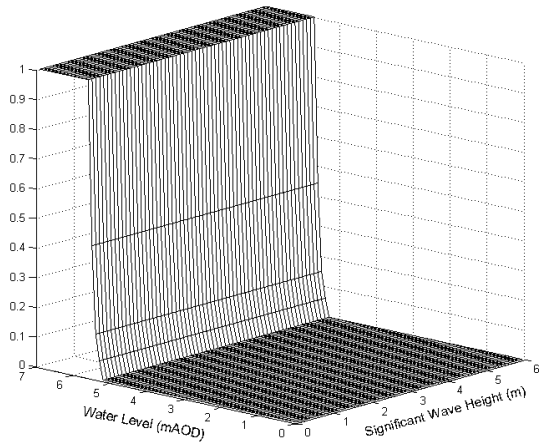

4 – Piping

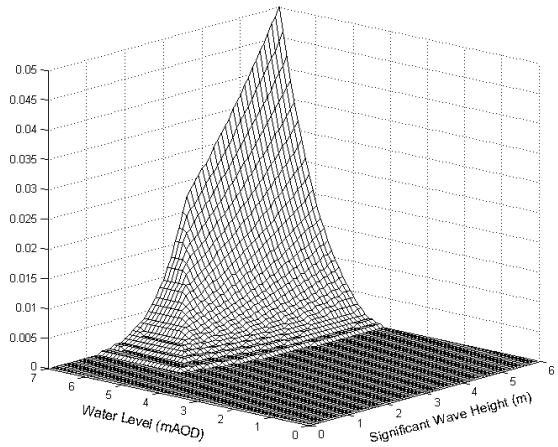

D – Rock armour

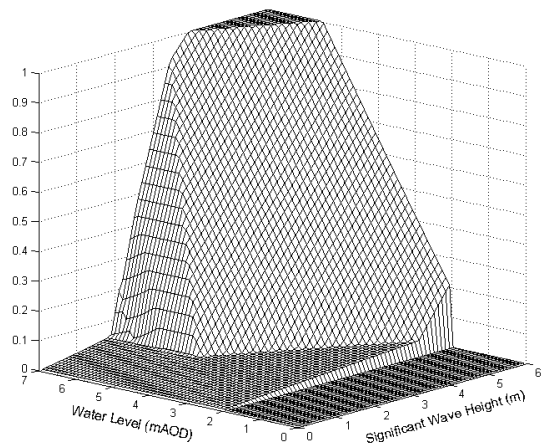

K – Dune erosion

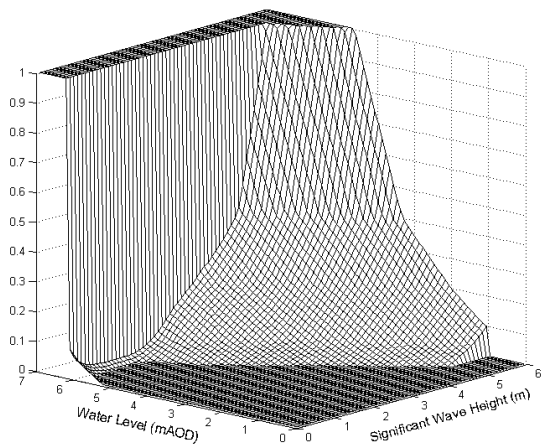

I – Shingle beach erosion

Figure 3.7 Failure probability distributions for defences C, D, I and K

Approximately 2000 loading points (combinations of H_s and W) were analysed, resulting in over 10,000 inundation model runs as the majority of loading points require more than one simulation to ensure all defence failure contributions that provide a non-negligible contribution towards

$$\sum_{k=1}^{n} P(D_k \mid H_s, W) = 1$$

are considered. For example, for H_s=2m and W=2m, 99% of this probability comes from the no defence failure scenario, whilst for H_s=4.5m and W=5m, 30 model runs are needed to capture 90% of this probability.

The convergence of the EAD is plotted in Figure 3.11. The final distribution of flood risk is shown in Figure 3.10 and gives a total flood risk in terms of EAD as £84,000; approximately twice the value of the initial assessment (Figure 3.9). The points were sampled from the density function $f_{imp}(H_s,W)$ taking the form of $R(H_s,W)$. In order to increase efficiency, the density of sampling was controlled such that H_{si}-H_{sj} and W_i -W_j

are always on a sampling grid of a manually controlled spacing. This was set at 0.05m. After the risk contribution from each loading point was analysed the distributions of $R(H_s,W)$ and consequently $f_{imp}(H_s,W)$ were updated.

There are a number of queries that can be made on the risk assessment output.

(a) The spatial distribution of flood risk in the floodplain can be obtained by calculating the total flood risk associated with each DEM cell, R_c, for m load samples is:

$$R_C = \sum_{i=1}^{m}\sum_{k=1}^{r} P(D_k \mid H_{si},W_i).P(H_{si},W_i).E_{kc} \tag{10}$$

where E_{kc} is the economic damage in the cell for the kth failure scenario.

(b) The spatial distribution of inundation probability in the floodplain (shown in Figure 3.13) obtained by calculating the inundation probability of each DEM cell, P_c, for m load samples is:

$$P_C = \sum_{i=1}^{m}\sum_{k=1}^{r} P(D_k \mid H_{si},W_i).P(H_{si},W_i) \tag{11}$$

(c) The relative contribution towards the EAD resulting from defence sections breaching is calculated by assuming the flood risk for each breaching failure combination is shared between the defences breaching. This is not a precise calculation as it assumes that flooding from each breached defence contributes equally to the flood risk for that failure combination. For instance, near the breaches the flood depth is likely to be controlled by the respective breach, however, in grid cells where contribution towards the impact is influenced by both breaches the relative contributions are unknown. Whilst not precise, this output still provides useful information about the contribution towards flood risk of the defence system.

(d) The risk contribution from storms of a given combination of wave height and water level or a specific return period are calculated using:

$$R(H_s,W) = \sum_{k=1}^{r} P(D_k \mid H_s,W).P(H_s,W).E_k \tag{12}$$

(e) The number of properties at risk of flooding to a given depth for a given probability (*eg*. in Towyn, 193 houses will be inundated up to a depth of 0.5m with a probability of 0.01).

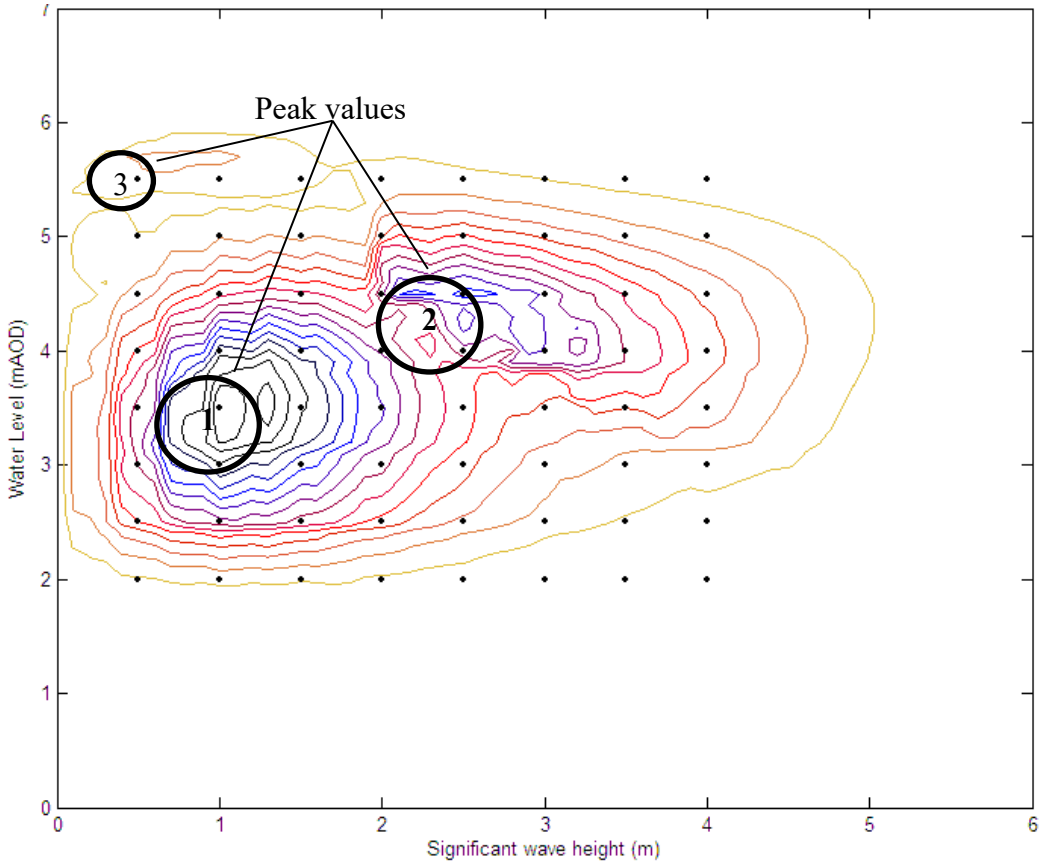

Figure 3.8 **A contour plot of $P(D_s|H_s, WL).f(H_s, WL)$ where darker contours represent higher values. The circles mark the approximate locations of peak values. The dots mark the initial sample points**

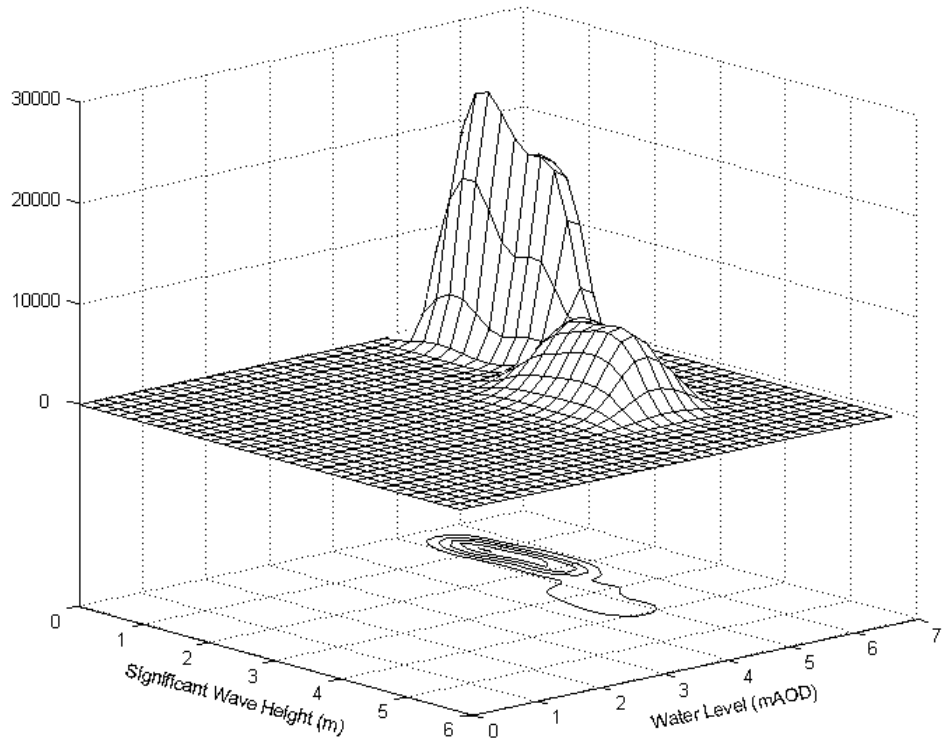

Figure 3.9 Initial surface describing the risk contribution for joint wave height and water level storm events based on only the initial 64 sample points

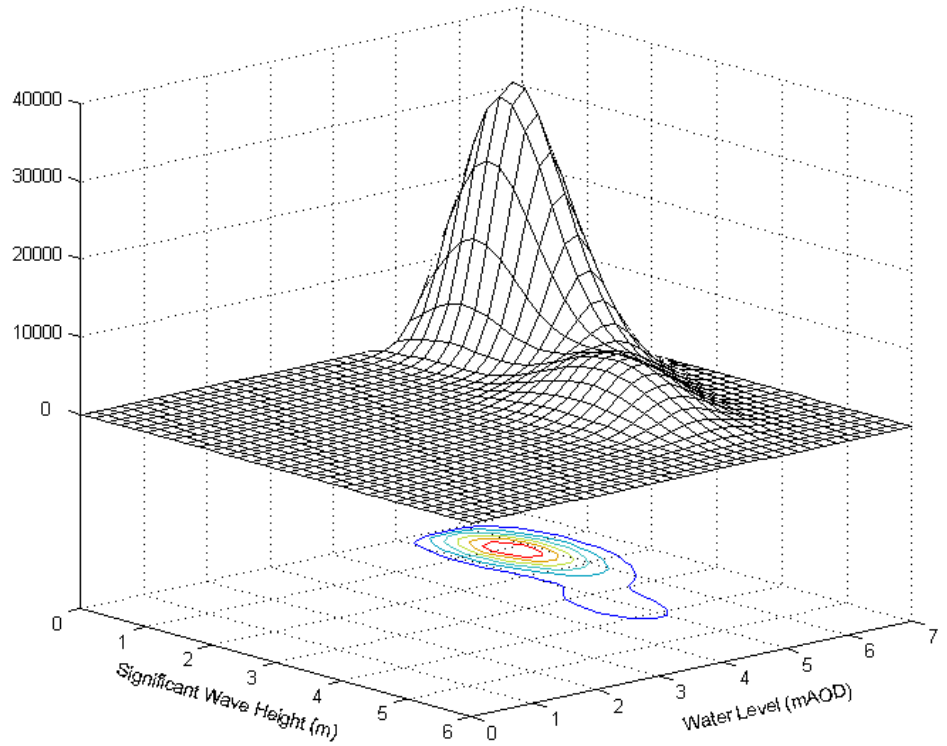

Figure 3.10 Final surface describing the risk contribution for joint wave height and water level storm events

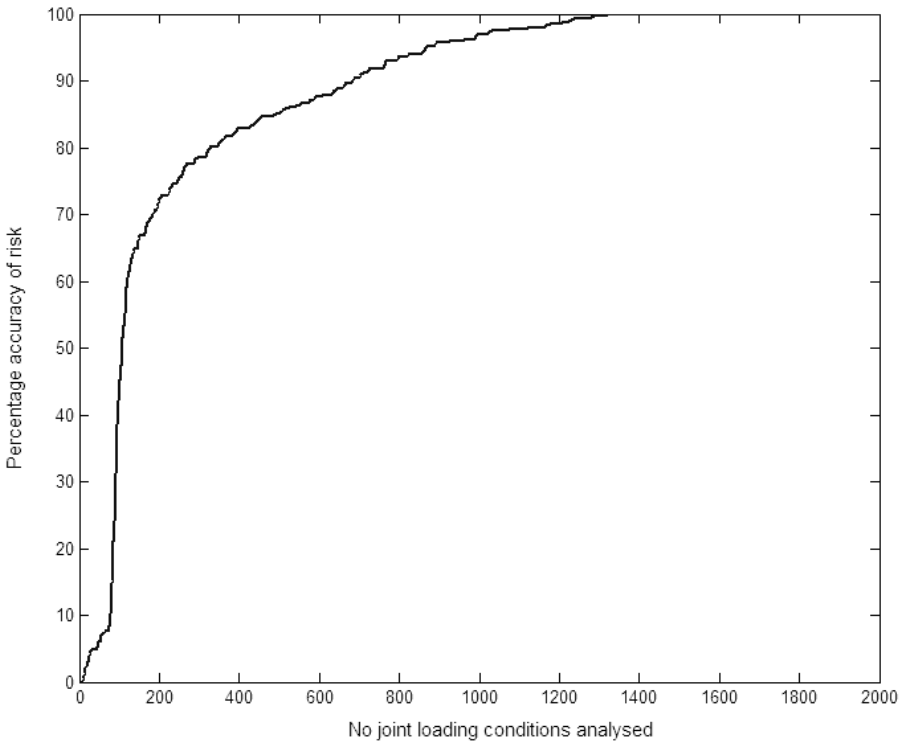

Figure 3.11 The convergence of the value of flood risk as a function of the number of loading points analysed

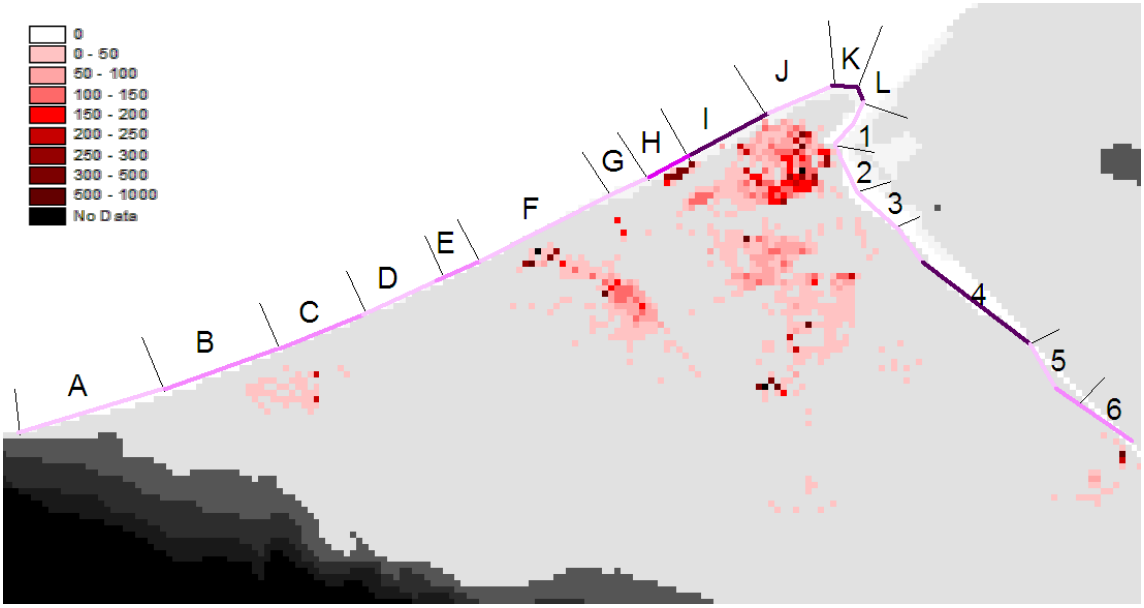

Figure 3.12 Spatial distribution of flood risk (in £s) with defence line shaded to represent contribution of defence towards flood risk (in £s) where darker shades represent a greater contribution

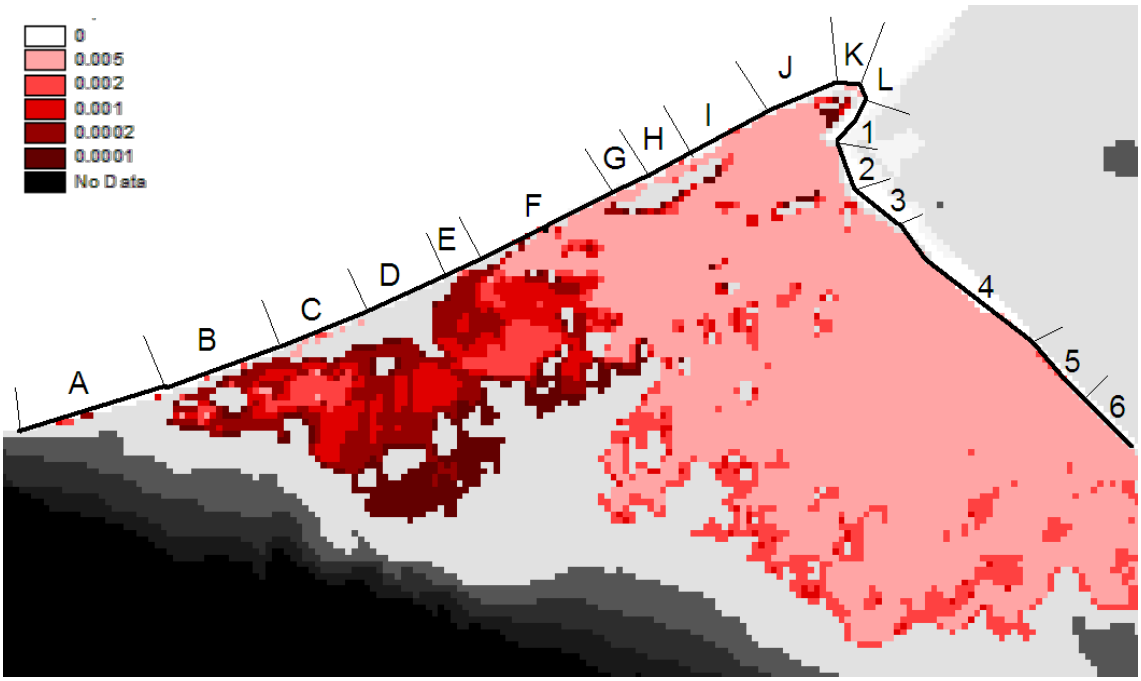

Figure 3.13 Spatial distribution of inundation probability with darker shades representing lower inundation probability

3.10 Discussion of insights from coastal case study application

A surface describing the economic flood risk conditional on wave height and water level has been generated. The surface stabilises after approximately 1500 loading

conditions have been analysed. This stabilisation occurs because additional inundation model runs provide little additional contribution to flood risk, thereby resulting in insignificant changes to the flood risk surface, and hence its integral. Using a 2.5GHz PC this takes less than 24 hours. However, it can be seen that the most immediate gain is in the first 2 hours (200 loading points) in which the risk estimate is calculated to within 75%. After approximately 12 hours the risk estimate is within 95% of the final value. In order to achieve this rate of convergence, an efficient sampling routine is required. Random Monte Carlo sampling of $H_s \times W$ would take significantly longer, as would sampling from a dense grid over the entirety of $H_s \times W$. However, methods developed to sensibly select regular grids could also be used to improve efficiency in the process.

The damage from the 1990 flood was estimated to be approximately £35million (~£50million in today's terms) (Roe, 1993). This is significantly larger than the EAD due to the level of protection provided by Towyn's defence system. There are a number of reasons for this. First, the £35million is not the EAD but is equivalent to the economic damage resulting from the failure of defence F as a result of an extreme event. Therefore in 1990, the contribution towards the total EAD from this particular event would be substantially lower than £35million. However, the risk contribution from the failure of defence F in 1990 can not be directly compared to the corresponding risk contribution from this analysis as the defence system has undergone significant strengthening since the 1990 failure, resulting in reduced failure probabilities. A similar analysis in 1990 would output a higher EAD reflecting the contribution of this investment in flood defence infrastructure.

The results in themselves have demonstrated some interesting phenomena. The initial hypothesis that the greatest contribution to flood risk may lie near the maximum of the product of $P(D_s|H_s, W).f(H_s,W)$ (i.e. the design point) on initial inspection of Figure 3.14 may appear to be hopeful. This maximum (marked as peak 1 in Figure 3.8) occurs at $H_s \approx 1$m, $W \approx 3.5$m. This peak is dominated by the density of $f(H_s, W)$, whereas peaks 2 and 3 are dominated by the systems failure probability. At peak 2, the shape of the surface $P(D_s|H_s, W)$ is heavily dominated by the failure probabilities of defences K and L, whilst at peak 1, the contribution of other defences is greater, meaning the influence of defences K and L is less pronounced. For peak 3, the shape of $P(D_s|H_s, W)$ is mostly influenced by defences 4 and 6 as their failure is dominated by extreme water levels alone.

The topography at Towyn means that only a storm surge of greater than ~4m AOD will result in any inundation behind the defence system, whilst a surge of ~5m is required for damage to run into millions of pounds. Therefore, at Towyn it is not possible for inundation to occur under the loading conditions corresponding to the maximum of $P(D_s|H_s, W).f(H_s,W)$. Overtopping events at lower water levels do occur, but these do not release sufficient water into the floodplain to provide a substantial contribution towards flood risk. However, it can be seen in Figure 3.14 that the maximum point of flood risk occurs near peak 3 on the $P(D_s|H_s, W).f(H_s,W)$ surface. These observations confirm that whilst it is not unreasonable as a first assumption to assume that the maximum flood risk occurs near the maximum point on $P(D_s|H_s, W).f(H_s,W)$, there are other important contributory factors.

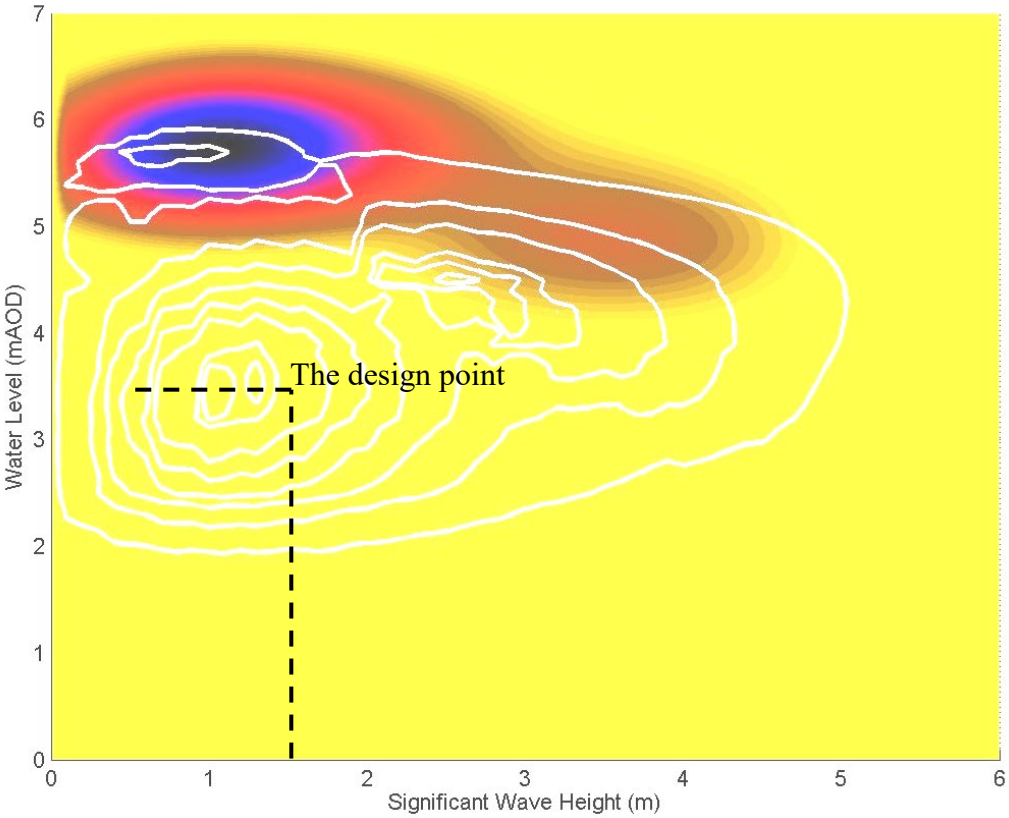

Figure 3.14 Contours defining the $P(D_s|H_s, W).f(H_s, W)$ surface that has been superimposed on the risk surface, with darker shades representing a greater risk contribution

The floodplain topography also influences the nature of the flood spreading. Figure 3.15 shows the flood outlines for four different defence failures for the same event (H_s=2m, W=5.5mAOD). The local topography dramatically influences the flood extent. Areas of high ground near a defence, for example behind defence C and L, restrict the volume of water that can flow into the floodplain. The narrow width of defence L (approximately 50m) further constricts the volume of water that can flow through it – even when fully breached. Conversely, defence 4 has a greater potential breach width and the lee side topography is such that water can flow into the floodplain unconstrained by patches of localised high ground.

However, upon reflection it is clear that the "The Design Point" is intuitively wrong. The resultant plot in Figure 3.14 indicates the sea condition at which "failure" is most likely to occur at the design point and suggests the fragility description and the definition of "failure" is wrong; perhaps it is overly influenced by the arbitrary small probability assigned in some of the failure modes.

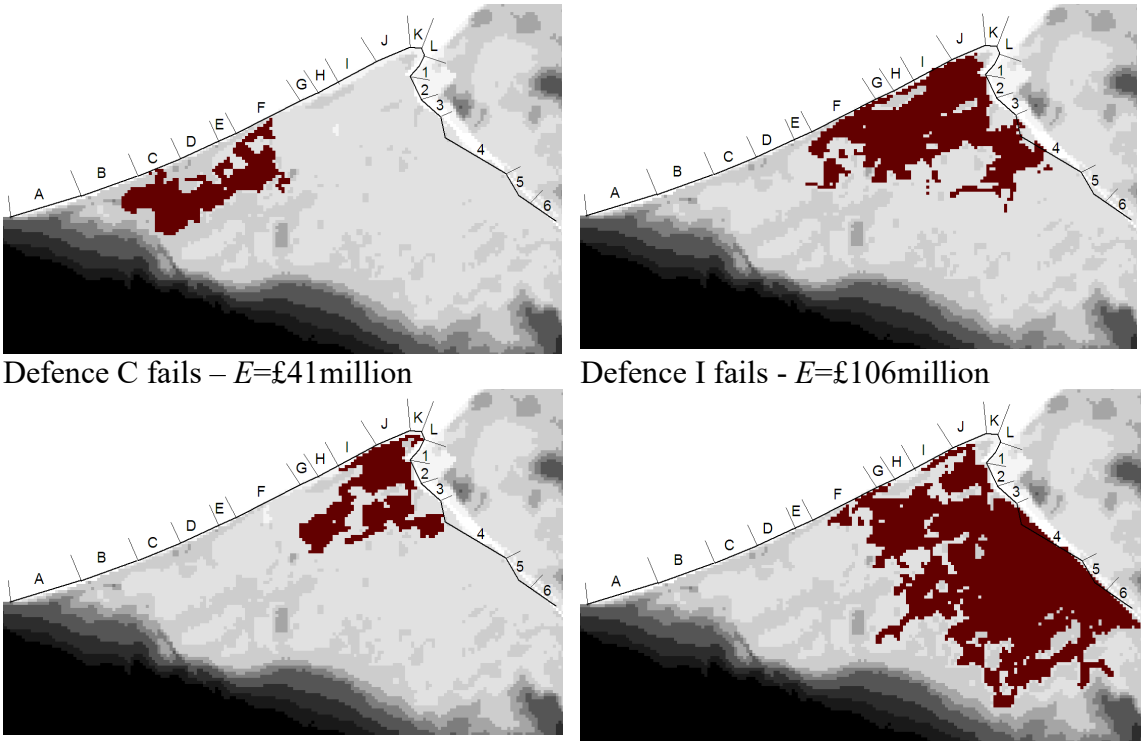

Defence C fails – E=£41million

Defence I fails - E=£106million

Defence L fails - E=£43million

Defence 4 fails - E=£79million

Figure 3.15 Flood outlines for the failure of defences C, I, L and 1 for H_s=2m, W=5.5mAOD

The floodplain topography at Towyn clearly influences the distribution of flood risk. However, the spatial distribution of floodplain assets in relation to the defences is also important. For example, failure of defence I results in the inundation of a large number of properties directly behind it. Whereas, failure of defences C, D or E will, excluding extreme storm surge events, result in the inundation of fewer properties. Therefore loading conditions that result in these defences contributing most towards any given point on $P(D_s|H_s, W).f(H_s,W)$ will result in a lower value of $R(H_s, W)$ than loading conditions that most likely cause the failure of defence I.

The risk space (Figure 3.10) has two peaks: the uppermost peak is dominated by the influence of water level, whereas the lower peak is influenced by joint wave and water level events. The greatest contribution towards $R(H_s, W)$ is under conditions of high water level and low wave height. This is due to a combination of the high failure probability of defences 4 and 6 under extreme water levels and the higher probability (relative to high wave height and water level events) of low wave height events. At the lower peak on $R(H_s, W)$, the greatest contribution towards these joint loading events is usually from the failure of defences K and L; this is a result of being fragile whilst resulting in high impacts when breached. The relative contribution of defence failure combinations towards $\sum_{k=1}^{n} P(D_k \mid H_s, W) = 1$ is important; if low impact events contribute the majority of this then $R(H_s,W)$ will be low. Therefore loading conditions that favour the failure of defence I over defence C will result in higher contributions towards flood risk.

The importance of higher order defence failures (*ie*. more than one defence failing) can also be observed. Under extreme loads, the contribution of these scenarios to flood risk for a given point on $H_s \times W$ can be more significant than single order failures. Table 3.11 lists a few examples of different defence failure combinations, their estimated economic damage and contribution to flood risk. This demonstrates how some defence failure combinations contribute towards flood risk for a given loading; in particular the contribution of multiple defence failures is more significant for extreme conditions. However, it should be noted that this is strongly influenced by the assumption of independence between defence section failure. Some defences, particularly those located near each other and sharing similar failure modes may not be completely independent – perhaps due to shared beach or defence properties. However, Van Gelder and Vrijling (1998) suggest that these types of spatial correlation may tend to zero over 50-100m. Examples of a number of loading combinations and their relative contributions towards flood risk are shown in Table 3.11.

Table 3.11 Examples of some of the defence failure combinations for two different loading scenarios and their contribution towards risk (note: not all defence failure combinations are listed for each loading scenario)

H_s (m)	W (m)	Defences failed	E_k	$R(D_k\|H_s,W)$
1.2	5.95	4 & 6	£114m	£29,200
1.2	5.95	4	£100m	£4,500
1.2	5.95	Total	£300m	£35,000
2.2	5	-	£0.018m	£83
2.2	5	H	£12m	£1,950
2.2	5	I	£46m	£2,110
2.2	5	B	£0.017m	£1
2.2	5	I & L	£45m	£500
2.2	5	H, K & L	£12m	£150
2.2	5	Total	£186m	£6,700
2.2	5.5	-	£0.025m	£96
2.2	5.5	K	£41m	£3,900
2.2	5.5	L	£43m	£4,200
2.2	5.5	K & L	£52m	£1,100
2.2	5.5	Total	£212m	£10,460

4. CONCLUSIONS

The need for improved risk assessment methodologies to support shoreline management planning has been identified. An efficient systems-based approach to assessing the risk associated with coastal defence failure has been proposed. The methodology takes advantage of robust level III techniques used to estimate extreme loading conditions. Appropriate response functions are selected for each defence in the system to estimate their probability of failure. An inundation model is used to generate realistic estimates of inundation depth and extent. The computational burden of a level III analysis is reduced through the use of importance sampling techniques. Whereas, traditional level II techniques estimate failure probabilities, this methodology samples the risk space.

The example implementation at Towyn in Wales demonstrates that the methodology provides an efficient and transparent means of assessing the flood risk of a complex defence system. However, the methodology provides more than just an EAD. The spatial distributions of flood risk and inundation probability are readily extracted, as is the relative contribution from each defence towards the total flood risk. The methodology also provides information on the response of the defences over a complete range of loads, enabling vulnerabilities in the system to be better identified. The contribution of multiple defence failures, which has been shown to be important under certain loading conditions, can be explored. Risk has been shown to be a complex function of joint loadings, beach response, defence(s) and their resistance, floodplain topography and the geographical location of impacts in the floodplain. This analysis, on top of providing the usual outputs such as EAD associated with traditional risk assessment techniques, has provided a more rigorous understanding of the system in terms of its vulnerabilities, beach and defence behaviour under different loadings and likely impacts. This methodology can be used to assist broad scale shoreline planners identify appropriate resource allocation strategies and test scenarios of changed storm surge frequency, investment in flood defence infrastructure and floodplain occupancy. It can also form the basis for a more detailed analysis and provide feedback to national scale risk assessments.

5. RECOMMENDATIONS

The development of the intermediate tier of the risk assessment methodology provides a significant improvement on RASP HLM which was constrained by the need for only nationally available datasets. However, a number of limitations of this methodology should be noted and given greater consideration in a more detailed analysis:

Science and method improvements

(a) antecedent loading conditions,

(b) fragility curve constructed from consideration of multiple defence failure modes,

(c) analysis of the dependence between defence strength parameters and between neighbouring sections,

(d) consideration of the influence on flooding of groundwater and surface run-off,

(e) more detailed analysis of the tangible and intangible impacts of flooding, including disruption to transportation systems,

(f) analysis of the influence of non-structural flood mitigation measures such as flood warning, and,

(g) analysis of the influence of human interventions (*eg*. defence reinforcement during flood events which has been shown to reduce the impact of some floods (Langemheem, 2002)).

Implementation improvements

(h) integration within the Modelling Decisions Support Framework in support of CFMPs;

(i) integration within specific decisions supports tools under development within PAMS;

(j) integration within specific decisions support tools to be developed in support of the identification of Flood Warning Flood Risk Areas;

(k) integration within specific decision support tools under development in support of the Agency regulation function;

(l) detailed links with NFCDD in support for future data collation and data management.

6. REFERENCES

BATES, P. D. and DE ROO, A.P.J. (2000). A simple raster-based model for flood inundation simulation, *Journal of Hydrology*, 236: 54-77.

CASCIATI, F. (1992), Risk analysis for marine systems: An introduction, *in Proc. Short Course on Design and Reliability of Coastal Structures*, *Venice, Oct. 1992*, pp 1-22, Tecnoprint snc, Bologna.

CASCIATI, F. and FARAVELLI, L. (1991). *Fragility Analysis of Complex Structural Systems*, Research Studies Press, Taunton.

CIRIA and CUR (1991), CIRIA Special Publication 83/CUR Report 154, *Manual on the use of rock in coastal and shoreline engineering*, CIRIA, London.

CIRIA (1996), *Beach management manual*, CIRIA R 153, London.

CUGIER, P. and LE HIR, P. (2002). Development of a 3D hydrodynamic model for coastal ecosystem modelling. Application to the plume of the Seine River (France). *Estuarine and Coastal Shelf Science*. 55 (5): 673-695.

CUR and TAW (1990), Vergeer, G.J.H.,(editor), *Probabilistic design of flood defences*, CUR Report 141, Balkema, Rotterdam.

CUR and TAW (1991), *Guide for the design of river dykes*, Vol 1 – Upper river, CUR/TAW Report 142, Balkema, Rotterdam.

DAWSON, R. J. and HALL, J. W. (2002a). Improved condition characterisation of coastal defences, *Proceedings of ICE Conference on Coastlines, Structures and Breakwaters*, pp 123-134, Thomas Telford, London.

DAWSON, R. J. and HALL, J. W. (2002b). Probabilistic condition characterisation of coastal structures using imprecise information, in *Coastal Engineering 2002, Proceedings of the 28th International Conference,* Cardiff UK, July 8-12, 2002, edited by J. McKee Smith. New Jersey: World Scientific, 2003. Vol.2: 2348-2359.

DAWSON, R. J. (2003), *Performance-based management of flood defence systems*, PhD Thesis, University of Bristol.

HALL, J. W., DAWSON, R. J., SAYERS, P., ROSU, C., CHATTERTON, J. and DEAKIN, R. (2003a). A methodology for national-scale flood risk assessment, *J. Water and Maritime Engineering*, 156(3): 235-247.

HALL, J. W., MEADOWCROFT, I. C., SAYERS, P. B. and BRAMLEY, M. E. (2003b). Integrated flood risk management in England and Wales, *Natural Hazards Review*, 4(3):126-135.

HAWKES, P. J., GOULDBY, B. P, TAWN, J. A. and OWEN, M. W. (2002). The joint probability of waves and water levels in coastal engineering, *J. Hydraulic Research*, 40(3): 241-251.

HORRITT, M. S. and BATES, P. D. (2001). Predicting floodplain inundation: raster-based modelling versus the finite-element approach, *Hydrological Processes*, 15: 825-842.

HR WALLINGFORD (1985). Conwy Estuary Crossing Field data collected by Hydraulics Research. Report EX 1251.

HR WALLINGFORD (1990). Joint probability of waves and water levels on the North Wales coast. HR Wallingford Report EX 2133.

HR WALLINGFORD (1999). *Overtopping of Seawalls: Design and Assessment Manual*, R&D Technical Report W178.

HR WALLINGFORD (2003). *Conwy Tidal Flood Risk Assessment, Stage 1 – Interim Report*, Report EX 4667, HR Wallingford.

HR WALLINGFORD AND LANCASTER UNIVERSITY (2000). The joint probability of waves and water levels: JOIN-SEA: A rigorous but practical new approach. HR Wallingford Report SR 537.

JCSS – Joint Committee on Structural Safety (1981), General principles on reliability for structural design, Int. Assoc. for Bridge and Structural Engineering.

LANGEMHEEM, W., van de (2002). Floods on river plains: specificity, needs and advances in flood forecasting flood warning and emergency management, in *Proc. 2nd MITCH workshop, Barcelona*, http://www.mitch-ec.net/workshop2/ws2-programme.htm.

MELCHERS, R. E. (1989), Importance sampling in structural systems, *Structural Safety*, vol 6, pp 3-10.

MELCHERS, R. E. (1999), *Structural Reliability Analysis and Prediction* (2nd Edition), Wiley, Chichester.

MEADOWCROFT, I.C., REEVE, D.E., ALLSOP, N.W.H., DIMENT, R.P. and CROSS, J. (1996). Development of new risk assessment procedures for coastal structures, *Proc. ICE Advances in Coastal Structures and Breakwaters '95*, Thomas Telford, London.

MOHAMED, M (2002). Embankment Breach Formation and Modelling Methods. PhD. Thesis, The Open University.

MOSER, D. A. (1997), The use of risk analysis by the US Army Corps of Engineers, *Proc Hydrology and Hydraulics Workshop on Risk-based analysis for flood damage reduction studies, California*, USACE.

PENNING-ROWSELL, E.C., JOHNSON, C., TUNSTALL, S.M., TAPSELL, S.M., MORRIS, J., CHATTERTON, J.B., COKER, A. and GREEN, C. (2003), *The Benefits of Flood and Coastal Defence: Techniques and Data for 2003*. Middlesex University Flood Hazard Research Centre.

POWELL, K. A. (1990), *Predicting short term profile response for shingle beaches*, HR Wallingford Report SR 219.

POWELL, K. A. (1993), *Model tests of replenished beaches using widely graded sediments*, HR Wallingford Report SR 350.

PROUDMAN OCEANOGRAPHIC LABORATORY (1997). Estimates of extreme sea conditions: Spatial analyses for the UK coast. POL Internal Document No 112.

PUGH, D. T. (1987). *Tides, Surges and Mean Sea-Level*, Wiley, Chichester.

REEVE, D. E. (1998). Coastal flood risk assessment, *J. Waterway, Port, Coastal and Ocean Engineering*, 124(5): 219-228.
ROE, G. M. (1993). The Towyn experience and lessons learned, in *Rising sea level and coastal protection seminar report*, Ulster Museum, Belfast 22nd April 1993, pp62-74, Oceanography Laboratories, University of Liverpool.

SILVERMAN, B. W. (1986), *Density estimation for statistics and data analysis*, Chapman and Hall, London.

TERZAGHI, K., PECK, R. B. and MESRI, G. (1996), *Soil Mechanics in Engineering Practice*, 3rd Edition, Wiley, New York.

USACE (1996), *Risk-based analysis for flood damage reduction studies*, Report EM1110-2-1619, United States Army Corps of Engineers, Washington.

USACE (2002), Coastal Engineering Manual, USACE, Manual EM 1110-2-1100. http://www.usace.army.mil/inet/usace-docs/eng-manuals/

VAN DER MEER, J.W. (1988), *Rock slopes and gravel beaches under wave attack*, PhD Thesis, Delft University of Technology. Also, Delft Hydraulics Communication No. 396.

VAN GELDER, P. H. J. M. and VRIJLING, J. K. (1998), The effect of inherent uncertainty in time and space on the reliability of flood protection, *Safety and Reliability: Proc. ESREL '98 Conf., Trondheim, Norway*, eds. S. Lydersen, G. K. Hansen and H. Sandtorv, pp451-456, Balkema, Rotterdam.

VOORTMAN, H. G. (2003), Risk-*based design of large-scale flood defence systems*, PhD Thesis, Delft University.

VOORTMAN, H.G., VAN GELDER, P.H.A.J.M, and VRIJLING, J.K. (2002), Risk-based design of large-scale flood defence systems, in *Coastal Engineering 2002,Proceedings of the 28th International Conference*, Cardiff UK, July 8-12, Vol.2: 2373- 2385, World Scientific, Singapore.

VRIJLING, J.K. (1993), Development in probabilistic design of flood defences in the Netherlands, in *Reliability and Uncertainty Analyses in Hydraulic Design*, B.C. Yen and Y-K Tung (eds.) pp133-178, ASCE, New York.

WAHL, T. L. (1998), *Prediction of embankment dam breach parameters: A literature review and needs assessment*, Dams Safety Office: DSO-98-004, also available at http://www.usbr.gov/pmts/hydraulics_lab/twahl/

ZERGER, A., SMITH, D. I., HUNTER, G. J. and JONES, S. D. (2002), Riding the storm: a comparison of uncertainty modelling techniques for storm surge risk management, *Applied Geography*, 22: 307-330.

Acknowledgements
The research described in this paper formed part of a project entitled "RASP: Risk assessment for flood and coastal defence systems for strategic planning", funded by the Environment Agency within the joint Defra/Environment Agency Flood and Coastal Defence R&D programme. Data used in the case study was kindly provided by The Environment Agency, Conwy Borough County Council and Dr. Mohamed Hassan of HR Wallingford. Dr Hall's research is funded by a Royal Academy of Engineering post-doctoral research fellowship.

7. BIBLIOGRAPHY

BUIJS, F.A., VAN GELDER, P.H.A.J.M., VRIJLING, J.K., VROUWENVELDER, A.C.W.M., HALL, J.W. and SAYERS, P.B. (2003). Application of Dutch reliability methods for flood defences in the UK, in *ESREL '03: Proceedings of the European Safety and Reliability Conference*, Maastricht, Netherlands, June 15 - 18, 2003, edited by T. Bedford and P.H.A.J.M van Gelder. Lisse: Balkema, 2003. pp.311-319.

BURGESS, K., BALSON, P., DYER, K. ORFORD, J. and TOWNEND, I. (2002). FutureCoast – The integration of knowledge to assess future coastal evolution at a national scale, in Cardiff UK, July 8-12, 2002, edited by J. McKee Smith. New Jersey: World Scientific, 2003. Vol.3: 3221-3233.

CIRIA (1986). *Performance of Sea Walls: Technical Note 126*, CIRIA, London.

COLEMAND, M. D. and MERCER, J. B. (2002). NEXTMap Britain: Completing Phase 1 of Intermap's Global Mapping Strategy, *GeoInformatics*, December 2002: 16-19.

ENVIRONMENT AGENCY (1996) *Risk Assessment for Sea and Tidal Defence Schemes*. Report 459/9/Y, Bristol.

GILL, J., WATKINSON, A. and COTE, I. (2004). *Linking sea level rise, coastal biodiversity and economic activity in Caribbean island states: towards the development of a coastal island simulator*, Tyndall Centre Technical Report 9: IT1.38 Final Report.

HALCROW, HR WALLINGFORD, JOHN CHATTERTON ASSOCIATES (2001). *National Appraisal of Assets at Risk from flooding and coastal erosion including the effects of climate change*, DEFRA, London.

HALL, J.W., LEE, E.M. and MEADOWCROFT, I.C. (2000). Risk-based benefit assessment of coastal cliff recession. *Water and Maritime Eng.* 142: 127-139.

HALL, J.W., MEADOWCROFT, I.C., LEE, E.M. and VAN GELDER, P.H.A.J.M. (2002). Stochastic simulation of episodic soft coastal cliff recession. *Coastal Engineering*, 46(3):159-174.

HALL, J. W., SAYERS, P. B. (2004). National-scale assessment of current and future flood risk in England and Wales, *Natural Hazards*, accepted.

HM TREASURY (2002). *Spending Review 2002*, Chapter 16, HMSO, London.

HR WALLINGFORD (1974). A55 Trunk Road Improvement, Hydrographic survey and hydraulic investigation of a bridge crossing near Deganwy. Report EX 651.

HR WALLINGFORD (1986). Conwy Estuary Crossing, Waves at the reclamation areas. HR Wallingford Report EX 1526.

HR WALLINGFORD (1986). Conwy Estuary Crossing Waves at the Reclamation Areas. Report EX 1526.

HR WALLINGFORD (1987). Conwy Estuary Crossing Waves at the Deganwy Jetty. Report EX 1532.

HR WALLINGFORD (1991). Colwyn Borough Sea Defence Review.

HR WALLINGFORD (1993). Mobile bed physical model study of proposed developments. HR Wallingford Report EX 2754.

HR WALLINGFORD, FHRC, CEH WALLINGFORD, EALES, R. and CRANFIELD UNIVERSITY (2002). Catchment Flood Management Plans: Development of a Modelling and Decision-Support Framework, Report EX4495, HR Wallingford. http://www.mdsf.co.uk/.

HR WALLINGFORD, UNIVERSITY OF BRISTOL, HALCROW and JOHN CHATTERTON ASSOCIATES (2003). *National Flood Risk Assessment 2002*, Report EX 4722, HR Wallingford.

LINFORD, T., JONES, Y., BARRETT, J. and BUTLER, G. (2002). National Flood and Coastal Defence Database, in *Coastal and River Eng: Proc DEFRA conf., Keele, 2002*, DEFRA.

MADRELL, R. J., REEVE, D. E. and HEATON, C. R. (1998). Establishing coastal flood risks from single storms and the distribution of the risk of structural failure, in *Proc. Coastlines, Structures and Breakwaters 1998*, Thomas Telford, London.

McGLADE, J. M. (2003). A diversity based fuzzy systems approach to ecosystem health assessment, *Aquatic ecosystem health and management*, 6(2): 205-216.

MELCHERS, R. E. (1999). *Structural Reliability Analysis and Prediction* (2nd Edition). Wiley, Chichester.

MOSBY, J. E. G. (1938). The Horsey flood, 1938: An example of storm effect on a low coast, in *Geographical Journal*, 93(5): 413-418.

SAYERS, P.B., HALL, J.W. AND MEADOWCROFT, I.C. (2002), Towards risk-based flood hazard management in the UK. *Proceedings of the Institution of Civil Engineers – Civil Engineering*, vol 150**,** Special Issue 1, 36-42.

STEERS, J. A. (1953). The East Coast Floods, *Geographical Journal*, Vol 119, No 3, pp 280-295.

WALKDEN, M.J.A and HALL, J.W. (2002). A model of soft cliff and platform erosion, in *Coastal Engineering 2002,Proceedings of the 28th International Conference,* Cardiff UK, July 8-12, 2002, Vol 3: 3333-3345, World Scientific, Singapore.